Dipolar effects in magnetic thin films and quasi-two-dimensional systems

K. De'Bell*

Department of Physics, Trent University, Peterborough, Ontario, Canada K9J 7B8

A. B. MacIsaac

Department of Applied Mathematics, University of Western Ontario, London, Ontario, Canada N6A 5B9

J. P. Whitehead

Department of Physics, Memorial University, St. John's, Newfoundland, Canada A1B 3X7

Thin films and quasi-two-dimensional systems show a wide range of ordering effects and related pattern-formation phenomena. The origins of these phenomena can often be traced to competition between the atomic (or molecular) interactions in the system and the resulting inherent frustration of the system. In magnetic thin films, a wide range of magnetic structures are possible as a result of the competition between the long-ranged dipolar interactions and localized interactions. This article reviews recent experimental and theoretical work which has developed our understanding of ordering and pattern formation in these films and in related structures.

CONTENTS

*Current address: Faculty of Science, Applied Science, and Engineering, University of New Brunswick at Saint John, St. John, New Brunswick, Canada E2L 4L5.

INTRODUCTION

Thin films and quasi-two-dimensional materials have many technological applications, including uses in electronics, data storage, and catalysis in the case of metal-on-metal films, and in biotechnology and pharmacology in the case of molecular films. Recent advances in film growth techniques such as atomic (or molecular) beam epitaxy and in characterization methods such as the surface magneto-optical Kerr effect provide not only an opportunity for further technological application but also allow one to consider thin films as an important testing ground of our understanding of atomic interactions. The development of materials with characteristics tailored to a specific application requires a detailed understanding of their microscopic interactions, how these interactions are affected by factors such as composition and preparation, and how they determine the material properties. For example, the use of ultrathin magnetic films for data storage requires that the magnetization of the film be set and read with a high degree of accuracy and spatial resolution. Variations in the composition of the film can be used to manipulate desired properties such as sensitivity to an external field (Weber *et al.*, 1995). The operating parameters for such devices are often predetermined or constrained, and hence the ability to ''design'' a material to meet these constraints and optimize performance can be of significant technological benefit.

Our purpose in this article is to show how, by bringing together existing experimental and theoretical results, one can understand the formation of ordered states in quasi-two-dimensional systems, including the pattern formation of structures consisting of domains with mesoscopic dimensions, in terms of a simple model of the magnetic interactions. Two systems are examined in some detail; these are ultrathin (i.e., a few atomic layers) metal films on metal substrates, and the rare-earth layers that occur in the perovskite structures of $REBa_2Cu_3O_{7-\delta}$, where RE represents a rare earth from the lanthanide series. The choice of these particular sys-

tems is motivated in part by the large number of experimental studies that have been performed on them in recent years. These studies have in turn been motivated both by the technological importance of these systems and by the insight that they provide into the fundamental role of interactions at the atomic level in determining macroscopic magnetic properties. Both experimental and theoretical studies have revealed several unusual magnetic properties of these systems. These include an initial increase in the static magnetization with increasing temperature in the presence of an external magnetic field (see Sec. V.E) and the presence of a frequency-dependent peak and exponential decay with increasing temperature of the real part of the ac susceptibility (see Sec. V.B.3).

A realistic theoretical description of these systems must include the exchange interaction, the dipolar interaction, and the on-site magnetocrystalline anisotropy, since the appearance of long-range magnetic order in quasi-two-dimensional systems requires the breaking of the symmetry by the magnetic anisotropy. The detailed nature of the magnetic anisotropy is determined by a subtle combination of the magnetocrystalline interactions, due to the structure of the crystal or presence of a surface, and the dipolar interaction, which is inherently anisotropic.

The dipolar interaction, which is often ignored in theoretical studies of magnetic systems, plays an essential role in stabilizing long-range magnetic order in two-dimensional systems, as well as in determining the nature and morphology of the ordered state. In addition to the inherent anisotropy of the dipolar interaction, its long-range character is also important in determining the magnetic properties of these materials. As discussed in the later parts of the article, it is the interplay between the on-site, short-range, and long-range interactions that results in the rich variety of magnetic properties of these systems. This is true of both the relatively simple single, ordered phases exhibited by the layered rare-earth systems and of the more complex multiple, ordered phases and pattern formation exhibited by the ultrathin metal films.

The formation of ordered states, which are dependent on the long-range character of the dipolar interaction, including states with mesoscopic domain patterns, is a much wider phenomenon than the particular systems we have chosen to focus on in this review. Indeed, this behavior is characteristic of a variety of quasi-two-dimensional systems (Seul and Andelman, 1995). In this sense, the studies discussed in this article provide insight into a much wider class of physical systems than just our two particular examples.

The outline of this review article is as follows: After the introduction we present a summary of some of the key experimental results for both magnetic thin films and the $REBa_2Cu_3O_{7-\delta}$ compounds in Sec. II. These experiments form the basis of much of the remainder of the article, which is primarily concerned with examining the extent to which theoretical and numerical studies can provide a reasonable account of the observed properties in terms of the magnetic interactions at the atomic level. We also seek to determine how systems belonging to the same general structural family, but containing different components, can be treated systematically.

The long-range character of the dipolar interaction requires some adaption of certain theoretical techniques. In Sec. III, we provide a brief overview of a method for performing the necessary lattice sums for ground-state energy calculations, and show how this summation technique is incorporated into finite-temperature Monte Carlo simulations to ensure a consistent treatment of finite-size effects.

The role of anisotropy, arising from both the magnetocrystalline interactions and the dipolar interaction, in ordering quasi-two-dimensional systems is most clearly revealed within the context of spin-wave theory, as discussed in Sec. IV. A notable result is that, even in the absence of magnetocrystalline anisotropy, the dipolar interaction stabilizes long-range order in two-dimensional planar systems with both ferromagnetic and antiferromagnetic ground states. This contrasts with systems that have exchange interactions only, which cannot exhibit long-range order in two dimensions.

Section V summarizes results obtained from theoretical models of the rare-earth layered systems and ultrathin magnetic films. These are compared with experimental results and the success of models using the three interactions described in detail below is assessed.

An intriguing property of ultrathin magnetic films is their ability to exhibit a reorientation transition. At this transition the magnetic moments of the film realign from an out-of-plane orientation to a (predominately) in-plane orientation as the temperature or film thickness is varied. Understanding this phenomenon is of great interest for fundamental studies of magnetic systems; however, it is also of considerable significance for applications such as data storage, where stability of the magnetic configuration is required. Section VI extends the comparison of theoretical and experimental studies to consider the reorientation transition.

Finally, in Sec. VII we discuss some open questions and areas for future study.

I. COMPETING INTERACTIONS IN FILMS

A. Exchange interactions

The simplest model of a two-dimensional magnetic system consists of a term corresponding to a short-ranged exchange interaction between nearest-neighbor pairs $\langle i,j\rangle$ of spins and an external magnetic field coupling to the spins only:

$$-\mathcal{H}_{\rm ex}=\sum_{\langle i,j\rangle} J\vec{\sigma}_i\cdot\vec{\sigma}_j+\vec{H}\cdot\sum_i \vec{\sigma}_i\,, \tag{1}$$

where σ_i is an n-component classical spin vector. (In this review we deal mainly with classical spin models; quantum effects are discussed in the context of spin-wave theory in Sec. IV). The possible ordered states for such a model are correspondingly simple.

We begin with the uniaxial (Ising) case in which the spins are represented by scalars having positive and negative values ($\sigma_i = \pm 1$); if the exchange constant J is positive, the only ordered state that occurs at low temperatures is a simple ferromagnet such that in the (fully) ordered state the spins are all aligned in parallel. If the exchange constant is negative, the only ground state for open lattices, such as the square lattice, is the simple antiferromagnet, in which all nearest-neighbor pairs of spins are antiparallel; an ordered state corresponding to this ground state forms at low temperatures.

Other lattice structures may complicate this picture in the case of a negative exchange interaction. For example, on a triangular lattice it is not possible to find an arrangement of spins that simultaneously minimizes the energy of all spin-spin interaction terms in the Hamiltonian. As a result of this frustration, the system is unable to order at any finite temperature.

For spins with rotational symmetry, spontaneous long-range order does not occur at any finite temperature if only the exchange interaction is present (Mermin and Wagner, 1996). In the case of the two-component spin (planar) system, a transition associated with vortex pairing does, however, occur at the Kosterlitz-Thouless transition temperature (Kosterlitz and Thouless, 1973).

B. Dipolar interactions

In all real systems there is, in addition to any short-ranged exchange interaction, a long-ranged dipole-dipole interaction always present between the magnetic moments. The contribution of this interaction to the system Hamiltonian is

$$\mathcal{H}_{\rm dd} = \frac{g}{2} \sum_{i \neq j} \left(\frac{\vec{\sigma}_i \cdot \vec{\sigma}_j}{r_{ij}^3} - 3 \frac{(\vec{\sigma}_i \cdot \vec{r}_{ij})(\vec{\sigma}_j \cdot \vec{r}_{ij})}{r_{ij}^5} \right), \tag{2}$$

where the sum is over all possible pairs of sites on the lattice and $\vec{r}_{ij}$ is the vector connecting site i to site j. In many theoretical studies of magnetic systems this dipolar interaction is neglected, the rationale for this being the small magnitude of the dipolar interaction relative to the magnitude of the exchange interaction. In quasi-two-dimensional systems, the dipolar interaction can play an essential role in determining the magnetic properties. In the case of systems with rotational symmetry, the dipolar interaction can stabilize long-range order at a finite temperature (Male'ev, 1976). Moreover, the dipolar interaction between any two spins on the lattice not only decays slowly with distance but also depends on both the relative orientation of the two spins and their orientation relative to the vector joining the two sites. Consequently the ground state of a system determined by the dipolar interaction alone differs from the ground state of a system determined by the exchange interaction alone. When both interactions are present the system is inherently frustrated.

As we shall show below, many interesting properties of systems with dipolar interactions result from this inherent frustration of the system. In particular, the subtle interplay between the localized exchange interaction and the relatively weak but long-range dipolar interaction can give rise to magnetic structures on a mesoscopic length scale. This interplay between long-range and short-range interactions manifests itself in pattern formation in a wide range of physical systems (Seul and Andelman, 1995). The structure factor (see Sec. V.C) characterizes the morphology and symmetry of the pattern structure. It provides a useful way of identifying analogies between systems that form patterned structures.

Another important property of the dipolar interaction for two-dimensional films is that it breaks the symmetry between the out-of-plane orientation of the spins and the in-plane orientation of the spins in the ordered state. For a system with dipolar interactions only, the ground state for spins arranged on a square lattice has all of the spins oriented in the plane of the film (see Sec. III.B).

C. Magnetocrystalline anisotropy

In addition to exchange and dipolar spin-spin interactions, and coupling to an external applied magnetic field, spins in a magnetic system may experience a localized (on-site) anisotropy due to interaction with the crystal environment. Therefore, in general, a thin magnetic film is described by a Hamiltonian,

$$\mathcal{H} = \mathcal{H}_{\rm ex} + \mathcal{H}_{\rm dd} + \mathcal{H}_{\rm an}. \tag{3}$$

For many systems of interest, the magnetocrystalline anisotropy may be represented by a term in the Hamiltonian:

$$\mathcal{H}_{\rm an} = \sum_i \sum_{\alpha\beta} A_{\alpha\beta} \sigma_i^\alpha \sigma_i^\beta, \tag{4}$$

where i labels the lattice site and α and β denote Cartesian components.

The simplest example of such an anisotropy is the crystalline-electric-field (CEF)-induced anisotropy in the heavy rare earths. In the lowest-order representation the anisotropy fields can be written in terms of Steven's operators (Hutchings, 1964). This representation is adequate for the description of magnetocrystalline anisotropy in many rare-earth systems, including the quasi-two-dimensional layered rare-earth compounds discussed in the following sections (De'Bell and Whitehead, 1994). However, for transition metals such as those typically used in the thin metal films discussed in this review, *ab initio* or band-theory calculations may be required to calculate the nature of the anisotropy in a material (see, for example, Lorenz and Hafner, 1995, and references therein).

In bulk systems, deviations from cubic symmetry (e.g., by tetragonal or orthorhombic lattice structures) may result in a reduced symmetry for the magnetocrystalline anisotropy and hence in ordering parallel to a particular axis or in a particular plane; thus justifying the treatment of the system by a uniaxial or planar model. Néel (1954) recognized that this effect would be particularly significant at a surface, as the presence of the surface breaks

TABLE I. Anisotropy energy K_2 (see Sec. VI) of fcc(001) and fcc(111) monolayers. Energies are expressed in meV/atom (Bruno, 1989). Numbers in brackets are the number of $3d+4s$ electrons for the elements shown.

N_v	(001)	(111)
Fe(8)	0.00	−0.61
Co(9)	−1.98	−2.47
Ni(10)	−0.86	−0.43

the symmetry in the bulk and distinguishes the direction perpendicular to the plane from directions in the plane of the surface. There has been a considerable effort to calculate the magnitude of the resulting surface anisotropy both by band-theory/spin-orbit calculations[1] and by *ab initio* calculations.[2] In Table I we quote the order-of-magnitude estimates obtained by Bruno (1989) for an isolated monolayer to give a sense of the size of this effect.

An extremely detailed experimental study and comparison with theory of the relative strengths of the dipolar and magnetocrystalline anisotropies in Co on Ag (001) has been performed by Bland *et al.* (1995). In this system, the magnetocrystalline anisotropy is dominant in determining the in-plane orientation of the magnetic moments and in introducing a gap in the spin-wave spectrum.

For a review of experimental studies of anistotropies in ultrathin films, the reader is referred to the article by Heinrich and Cochran (1994). This article also gives a detailed discussion of models of exchange interactions and on-site anisotropies.

In Sec. VI we shall return to the role that competition between this surface anisotropy term and the inherent anisotropy of the dipolar interaction plays in driving the reorientation transition that is observed in metal-on-metal films.

II. EXPERIMENTAL STUDIES

A. Magnetic thin films

The remarkable improvement in the ability to grow and characterize metal films of a few atomic thicknesses on metal substrates that has occurred in the past decade (Jones and Venus, 1994; Prutton, 1994) has led to a series of exciting observations regarding the character of the magnetic domains in such films. In a key early study in this series, Pappas *et al.* (1990) studied a number of films of iron (Fe), each approximately three atomic layers thick, deposited on copper [Cu(100)]. Using spin-polarized electron spectroscopy they found that the magnetic moments of the Fe atoms were aligned perpendicular to the plane of the film in the low-temperature regime. On heating, the sample was observed to pass through a region in which the net magnetization was lost but reappeared at still higher temperatures with a significant component in the plane of the film. Immediately above the onset of a net magnetization in this region, a smaller component in the perpendicular direction was also observed (Fig. 1). These changes in the magnetization occurred in a temperature range of $T \leqslant 350$ K in which the film was structurally stable. All of the changes in this region were reversible. At temperatures above 350 K there was an irreversible loss of magnetization that appeared to be associated with a structural transition at approximately 300 K.

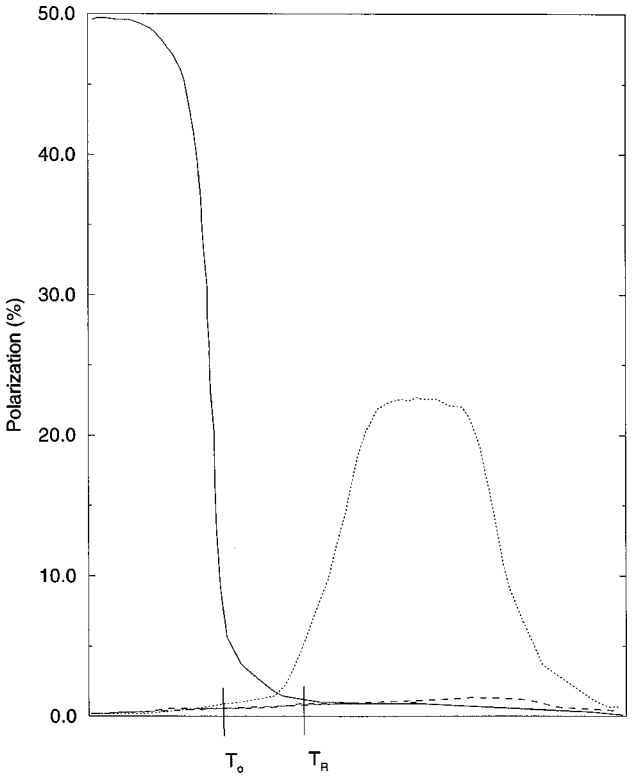

FIG. 1. Schematic representation of the out-of-plane and in-plane magnetization curves observed by Pappas *et al.* (1990): solid curve, the out-of-plane magnetization; dotted and dashed curves, the two in-plane magnetizations.

Pappas *et al.* (1990) interpreted their observations in the structurally stable region as a switching transition from a uniaxial state perpendicular to the plane of the film, due to interfacial anisotropy at low temperatures, to a canted magnetic state above the transition. They noted two possible explanations for the region of demagnetization between the perpendicular and canted phases. The first possibility was that the region was truly paramagnetic as a result of the demagnetizing fields exactly canceling the interfacial anisotropy and thereby restoring rotational symmetry. The second possibility was that the magnetic structure in this region was one of static domains with zero net magnetization. Pappas *et al.*

[1]See, for example, Bruno, 1989; Pick and Dreyssé, 1992; Pick *et al.*, 1994; Lessard *et al.*, 1997.

[2]See, for example, Gay and Richter, 1986, 1987; Daalderop *et al.*, 1990, 1991; Li *et al.*, 1990; Daalderop *et al.*, 1992; Victoria and MacLaren, 1993; Wang *et al.*, 1993a, 1993b; Szunyogh *et al.*, 1995.

(1990) also noted that the temperature at which the switching transition occurred decreased as the film thickness increased.

The nature of the switching transition and the nature of the magnetic state in the vicinity of the transition was clarified by exacting experiments using scanning electron microscopy with polarization analysis. This technique allows imaging of magnetic structures on micrometer scales.

In a scanning-electron-microscopy study of cobalt (Co) on gold [Au(111)], Allenspach *et al.* (1990) demonstrated the dependence of magnetic structure on film thickness at a constant temperature of 300 K. At three atomic layers thickness the magnetic moments were aligned perpendicular to the plane; however, the moments were arranged in irregularly shaped domains. As the film thickness increased, the moments of the domains rotated continuously until at five atomic layers the magnetic moments were almost entirely parallel to the plane of the film.

Allenspach and Bischof (1992) also used scanning electron microscopy to study the variation of domain structure with temperature in fixed-thickness films of Fe/Cu(100). Below a characteristic temperature, the moments form a single magnetic domain oriented perpendicular to the plane of the film. As the temperature is increased above this characteristic temperature, the moments remain predominately perpendicular to the plane but domains of reversed moment form. These domains are elongated, and the elongation is aligned along a crystallographic direction. As the temperature continues to increase, the magnetic moments reorient from the perpendicular direction to a direction parallel to the plane of the film.

Berger and Hopster (1996a, 1996b) have studied the remnant magnetization in Fe films of approximately four monolayers (4ML) on a silver [Ag(100)] substrate. Their observations of the (near) zero-field, perpendicular, and parallel-to-plane magnetizations are consistent with those of the earlier studies. The magnetization is perpendicular to the plane at low temperatures, with an intermediate region in which the perpendicular component of the magnetization rapidly decreases but the component of magnetization parallel to the plane remains zero until a higher temperature T_R is reached. At temperature T_R a net magnetic moment parallel to the plane of the film appears; this rapidly saturates with increasing temperature. For a 3.8ML film with $T_R = 370 \pm 10$ K, Berger and Hopster (1996a) found that the zero-field remnant magnetization was essentially zero in a temperature range 316 K $\leqslant T \leqslant$ 363 K. However, small applied magnetic fields $H = O(10\,\mathrm{Oe})$ were sufficient to restore the perpendicular magnetization to its saturation value. The critical field at which saturation occurs decreases with decreasing temperature. Moreover, Berger and Hopster observed that the shape of the dM/dH curve depends on temperature. At $T = 316$ K the curve has two clearly defined sharp peaks. As the temperature is increased, the peaks are suppressed and at temperatures close to T_R the dM/dH curve exhibits a single flat step. Although no hysteresis was observed in this temperature range ($T > 316$ K), at temperatures $T < 316$ K noticeable hysteresis effects were present.

Berger and Hopster's studies of the effect of magnetic fields on the remnant magnetization provide some insight into the stability of the domain phases. Evidence of metastability at low temperatures was obtained by applying a 90-Oe field to a 4ML film to saturate the magnetization in the perpendicular direction (Berger and Hopster, 1996b). The applied field was switched off and the time dependence of the perpendicular magnetization observed at various temperatures below $T_R \approx 210$ K. When the sample had previously been warmed from low temperatures in zero field it exhibited a loss of perpendicular magnetization at $T^* \approx 120$ K. However, when initially saturated by the 90-Oe field and then allowed to relax at fixed temperature, it exhibited relaxation to a nonzero remnant magnetization in a temperature range $102\,\mathrm{K} \geqslant T \geqslant 170\,\mathrm{K}$ with a finite relaxation time given by

$$\tau \approx \exp(E/k_B T) \tag{5}$$

with $E \approx 3.4$ eV.

A recurring problem in experimental studies of the magnetic properties of thin films is structural instability with respect to changes of temperature or changes of film thickness (see Li *et al.*, 1994; Baudelet *et al.*, 1995, and references therein). The importance of the physical structure of the film in determining the magnetic domain structures has been demonstrated by Speckmann *et al.* (1995) in studies of as-grown and annealed Co on Au(111) samples. Some progress has been made in attempting to isolate the effects of parameters such as temperature and film thickness on the magnetic properties by a careful choice of substrate. For example, Arnold *et al.* (1997) have grown fcc iron films on a substrate obtained by depositing two monolayers of nickel on the tungsten (110) surface. The underlying bcc tungsten (110) surface had some effect in that the resulting strain produced a twofold symmetry for in plane orientations of the iron moments; however, the film structure was stable in a range of 1–3 ML for temperatures below 400 K. Using susceptibility measurements based on the magneto-optical Kerr effect Arnold *et al.* (1997) found that, for films with less than approximately 2ML of iron, no reorientation transition was observed, but the transition from out-of-plane domains to a disordered state occurred directly as the temperature was increased. At higher coverage, the films exhibited a reorientation transition to an in-plane ferromagnetic phase before disordering. By extrapolation of their data lines for the order disorder transition and the reorientation transition, Arnold *et al.* (1997) identified a multicritical region. A schematic representation of the phase diagram obtained by Arnold *et al.* (1997) is shown in Fig. 2.

The experimental studies described above identify the key features of magnetic thin films that theoretical models must contain. Anisotropy is necessary to produce an ordered state in two-dimensional systems; however, the anisotropy in these films does not determine a single easy axis or plane at all temperatures. Typically, the

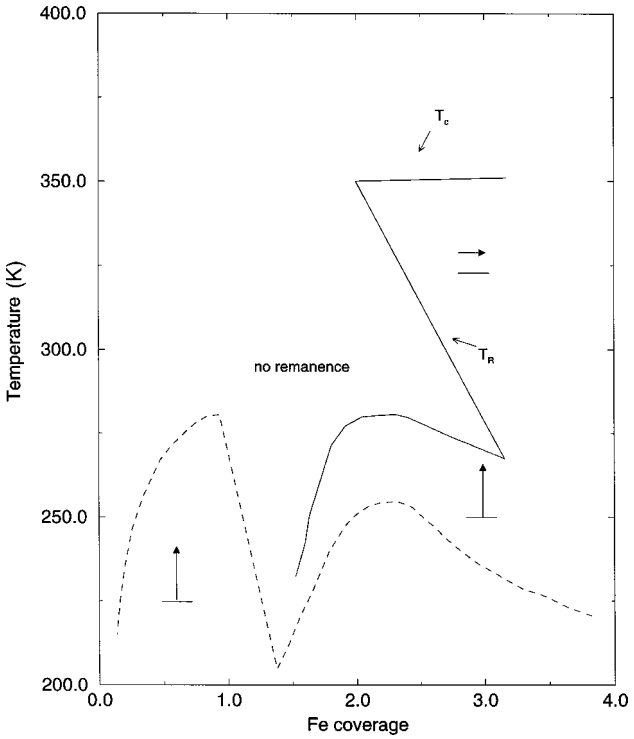

FIG. 2. Schematic representation of the phase diagram obtained by Arnold *et al.* (1997).

magnetization is perpendicular to the plane of the film at low temperatures, but at a finite temperature a reorientation occurs and the magnetization realigns in the plane of the film. [An exception to this is the Ni on Cu (001) system, which has in-plane ordering for thin films at low temperatures and which reorients out of plane above a critical temperature or film thickness (Schulz and Baberschke, 1994)]. In an intermediate range of temperatures below the reorientation transition temperature, both the perpendicular and in-plane components of the magnetization essentially disappear. The reorientation transition temperature is dependent on the thickness of the film. Finally, the work of Berger and Hopster indicates the existence of states that are close in energy to the domain ground states and that are metastable at low temperatures. The signature of these metastable states in the relaxation of the magnetization vanishes as the reorientation transition temperature is approached. We defer further comparison of these and other experimental magnetic thin-film studies with theory until the appropriate parts of Secs. V and VI.

B. Layered rare-earth systems

A considerable number of experimental studies have been performed on the magnetic properties of the rare earths in the family of compounds with general formula $REBa_2Cu_3O_{7-\delta}$. These compounds are derived from the parent compound $YBa_2Cu_3O_{7-\delta}$ by substituting the yttrium (Y) with one of the rare earths, typically from the lanthanide series, which we have denoted by RE. The interest in these compounds arises because the $YBa_2Cu_3O_{7-\delta}$ belongs to the class of high-T_c superconductors. $YBa_2Cu_3O_{7-\delta}$ has a perovskite crystal structure; the ab planes of yttrium ions each lie between two double copper oxide layers. For small values of the oxygen deficiency δ, the yttrium lattice is orthorhombic and the compound is superconducting, with a superconducting transition temperature $T_c \approx 90$ K. At sufficiently high values of the oxygen deficiency ($\delta \approx 1$) the yttrium lattice is tetragonal and the compound does not exhibit superconductivity but is instead an insulator. In both the orthorhombic and tetragonal crystal structures the separation of nearest-neighbor yttrium ions in the ab plane is approximately 4 Å, while the separation of the yttrium-ion planes in the c direction is approximately 12 Å.

Replacement of yttrium (Y) by the rare earths cerium (Ce), praseodymium (Pr), promethium (Pm), or terbium (Tb) destroys the superconducting nature of the sample for sufficiently high concentrations of the substituting rare earth (Maple *et al.*, 1987). However, complete substitution for the yttrium of the Kramers ions neodymium (Nd^{3+}), samarium (Sm^{3+}), gadolinium (Gd^{3+}), dysprosium (Dy^{3+}), or erbium (Er^{3+}) has little effect on the superconducting transition temperature, indicating that the magnetic moments are interacting only weakly with the superconducting electrons. These rare-earth compounds are also interesting because they order magnetically at low temperatures, typically $\leqslant 2$ K.

The fact that superconductivity coexists with the magnetic moments of the heavier rare earths is quite remarkable, but not unusual, as there exist a number of other magnetic superconductors, such as the $RERh_4B_4$ and $REHo_6S_8$ series of compounds, which have been extensively studied both theoretically and experimentally (Matsubara and Kotani, 1984). The fact that the lighter rare earths destroy the superconductivity is generally attributed to the mixed-valence nature of these ions.

These rare-earth compounds represent a fascinating class of magnetic compounds. The layered character of the perovskite crystal structure suggests that these are quasi-two-dimensional magnetic systems. The fact that substituting the heavier rare-earth ions for the Y ions has little effect on the superconducting transition temperature or the lattice spacing suggests that the rare-earth sublattice does not couple strongly to the oxide planes and may, to a first-order approximation, admit a systematic interpretation in terms of the Hamiltonian given by Eq. (3). Moreover, the low ordering temperatures of these compounds suggest that the dipolar interaction plays an important, if not dominant, role. Finally, there is the possibility that a detailed understanding of the magnetic properties of these compounds may be useful in revealing important aspects of superconductivity.

Early neutron-scattering experiments on composite samples of superconducting $ErBa_2Cu_3O_7$ confirmed that the system ordered antiferromagnetically at approximately 0.5 K with the moments aligned in the ab plane along the b axis. The moments are ordered ferromagnetically in the b direction and antiferromagnetically in

the *a* direction. (We refer to this as AF ordering.) However, these early experiments were unable to determine conclusively if the ordering was two- or three-dimensional. Further neutron-scattering experiments, just above the transition temperature, on high-quality single-crystal samples showed that the critical fluctuations consisted of rods, indicating no significant correlation in the *c* direction. This confirmed that the nature of the ordering was, in fact, quasi two dimensional (Lynn *et al.*, 1989). As the temperature is lowered below T_N, the magnetic ions would be expected to order along the *c* axis; however, the exact nature of the order along the *c* axis appears to be sample dependent and its precise determination is further complicated by the controversy that has surrounded the interpretation of these results (Malletta *et al.*, 1990; Clinton and Lynn, 1991b).

The neutron-scattering results on orthorhombic $ErBa_2Cu_3O_7$ are consistent with low-temperature specific-heat measurements, which showed that the specific heat was well fitted by the Onsager solution for the two-dimensional Ising model (Brown *et al.*, 1987; Nakazawa *et al.*, 1987; Simizu *et al.*, 1987; Lee *et al.*, 1988) and find that the critical exponent obtained for the order parameter was close to the expected value for a two-dimensional Ising model, $\beta=1/8$, but inconsistent with a value of $\beta\approx 1/3$ expected for a three-dimensional Ising or Heisenberg system. This observation of two-dimensional ordering may appear to be inconsistent with the long-ranged nature of the dipolar interaction; however, De'Bell and Whitehead (1991) showed that the coupling between moments in different planes, due to the dipolar interaction, is almost negligible.

In the case of the Er compound, the sharp Ising-like peak in the specific heat occurs only in samples with orthorhombic symmetry. If the oxygen deficiency is sufficiently reduced so that the rare-earth lattice is tetragonal, the sharp peak is replaced by a broad maximum (Nakazawa *et al.*, 1987; Simizu *et al.*, 1987; 1989). It is also found that the Er ions do not appear to order, even down to the lowest temperatures (Clinton *et al.*, 1995).

Experiments on $DyBa_2Cu_3O_7$ also show clear evidence of antiferromagnetic ordering with a Néel temperature of 0.95 K. However, unlike the Er compound, the spins are aligned along the *c* axis with the moments ordered antiferromagnetically in both the *a* and *b* directions (we refer to this as the AA phase). The critical scattering just above T_N is strongly 2D in character showing little correlation between the *ab* planes along the *c* axis (Clinton and Lynn, 1991a). The order parameter obtained from neutron scattering (Clinton and Lynn, 1991a) is relatively flat at low temperature and drops rapidly to zero close to T_N, in a manner qualitatively similar to that of the two-dimensional Ising model. This is consistent with specific-heat measurements which show a sharp Ising-like peak (Dirken and de Jongh, 1987; Allenspach *et al.*, 1995).

As the temperature is further reduced below T_N, three-dimensional order is observed; however, the precise nature of the ordering appears to depend strongly on the oxygen content and sample preparation, and, as with the measurements on the magnetic properties of $ErBa_2Cu_3O_7$, considerable controversy surrounded the interpretation of some of the early neutron-scattering data for $DyBa_2Cu_3O_7$. Recent experiments appear to have resolved the situation somewhat (Clinton *et al.*, 1995). In the case of a fully oxygenated compound, the spins appear to order antiferromagnetically along the *c* axis. On the other hand, for $\delta\approx 0.46$ the material is still in the superconducting phase, and the spins are aligned ferromagnetically along the *c* axis, with a transition temperature slightly lower than that of the fully oxygenated case, $T_N=0.87$ K ($T_N=0.91$ K).

The magnetic properties of the insulating phase $DyBa_2Cu_3O_6$ also show the effect of the degree of oxygenation on the nature of the magnetic ordering along the *c* axis. Neutron-scattering data indicate the existence of long-range antiferromagnetic order in the *ab* planes for $T<T_N$ with $T_N=0.55$ K. However, the magnetic order along the *c* axis appears to be short ranged and the magnetization does not appear to develop full three-dimensional order down to the lowest temperatures observed (Clinton *et al.*, 1995). Calorimetric studies are consistent with these observations in the sense that the heat-capacity measurements show sharp peaks for samples with large ($\delta\approx 1$) and small ($\delta\ll 1$) degrees of oxygenation, but the peaks are rounded for intermediate degrees of oxygenation.

Neutron-scattering experiments on $GdBa_2Cu_3O_7$ show that the Gd ions order antiferromagnetically at $T_N=2.2$ K. Like the $DyBa_2Cu_3O_7$, the magnetic moment of the Gd ions is aligned along the *c* axis and ordered antiferromagnetically along both the *a* and *b* axes. Specific-heat measurements on $GdBa_2Cu_3O_7$ show a peak at T_N (Brown *et al.*, 1987; Reeves *et al.*, 1987; Dunlap *et al.*, 1988) which can be described reasonably well by the 2D Ising model (van der Berg, 1987). However, it should be noted that the specific-heat curve exhibits a shoulder just below T_N (Brown *et al.*, 1987; Dunlap *et al.*, 1988). What is particularly notable in these results is that both specific-heat (Reeves *et al.*, 1987; Dunlap *et al.*, 1988) and neutron-scattering measurements indicate that the magnetic properties are virtually independent of the crystallographic structure (orthorhombic versus tetragonal).

While much of the work on the magnetic properties of the rare-earth compounds has focused on Dy, Gd, and Er, a number of interesting studies have been published on neodymium (Nd) and samarium (Sm). Early neutron-scattering work on the superconducting, orthorhombic phase of neodymium (Fischer *et al.*, 1989; Yang *et al.*, 1989), showed that the neodymium ions ordered antiferromagnetically with their moments aligned perpendicular to the plane. Heat-capacity measurements on both neodymium and samarium exhibited a sharp peak (Yang *et al.*, 1989) associated with magnetic ordering, and it was shown that the specific-heat curve was well fitted by the Onsager solution for the anisotropic 2D Ising model. While it is to be expected that the magnetic coupling along the *a* and *b* axes would differ, the coupling constants obtained from the "best fit" to the data differ by more than an order of magnitude in both cases

(Yang *et al.*, 1989; Allenspach *et al.*, 1995). It is difficult to account for such a large difference.

Also very interesting in the neodymium and samarium compounds is the fact that the sharp peak in the heat capacity is observed only in the orthorhombic phase. In the oxygen-deficient tetragonal phase the heat capacity has a much more ''rounded'' peak at a somewhat higher temperature than in the orthorhombic case (Yang *et al.*, 1989). More extensive results on the specific-heat measurements on $NdBa_2Cu_3O_{7-\delta}$ reveal a more complex relationship between the degree of oxygenation and the magnetic order (Allenspach *et al.*, 1995). As with the earlier results of Yang *et al.* (1989), for the fully oxygenated compound ($\delta \approx 0.07$), the heat capacity shows an Ising-like peak at the Néel temperature, and as δ is increased the peak shifts upward in temperature and initially becomes more rounded. However, Allenspach *et al.* (1995) also show that as δ is increased beyond 0.36 the peak begins to sharpen again. Allenspach *et al.* (1994) have had some success in fitting the specific-heat data to a simple cluster model for high oxygen content ($0<\delta<0.26$). However, for lower oxygen concentrations they claim the most appropriate model is ''inbetween a molecular field and a 3D Ising model.''

These results suggests that the degree of oxygenation has a significant effect on the magnetic properties of the rare-earth sublattice in $NdBa_2Cu_3O_{7-\delta}$. This is confirmed by neutron-scattering studies on $NdBa_2Cu_3O_{7-\delta}$ which show an interesting and unusual dependence on the degree of oxygenation. For $\delta=0.22$ the material is still superconducting; however, it does not appear to develop long-range magnetic order in the ab planes, but instead exhibits short-range 2D antiferromagnetic order with a correlation length that reaches a maximum value of around 22 Å (Clinton *et al.*, 1995). A further reduction in the degree of oxygenation to $\delta \approx 0.55$ destroys the superconductivity and appears to enhance the correlations along the c axis; however, long-range magnetic order does not develop down to the lowest temperatures. As suggested by the specific-heat measurements of Yang *et al.* (1989), long-range moloculer order is reestablished by a further reduction in the degree of oxygenation. At $\delta=0.7$ and $\delta=0.87$ the spins are ordered antiferromagnetically with transition temperatures $T_N=1.5$ K ($\delta=0.7$) and 1.75 K ($\delta=0.87$) but are tilted at 45° to the c axis.

There have also been extensive experimental and theoretical studies related to crystalline electric-field splitting in the $REBa_2Cu_3O_7$ compounds and their role in determining the magnetic properties of these compounds. These provide quantitative estimates of the magnetic-crystalline anisotropy, the ground-state magnetic moment, and the spin degeneracy at low temperatures. For a review and discussion of these properties the reader is referred to MacIsaac *et al.* (1992), Whitehead, De'Bell, and MacIsaac (1993), and De'Bell and Whitehead (1994).

III. THE DIPOLAR INTERACTION

In this section we briefly examine some important results in the calculation of the dipolar energy. In particular, the long-range nature and the anisotropic character of the dipolar interaction require considerable care in the evaluation of the dipolar contribution to the magnetic energy. We begin by examining a generalized form of the Ewald summation technique that provides a powerful means of dealing with the slowly convergent nature of dipolar sums. We then present the dipolar energy for a number of important spin configurations. Finally we present a widely used method for including the dipolar interaction in a Monte Carlo simulation.

A. Ewald summation technique

To include the dipolar interaction in any calculation, one needs a method of efficiently calculating the dipolar energy for particular spin configurations. The problem is complicated by the slowly convergent nature of the dipolar sums. Such summations are best treated using one of the variants of the Ewald summation technique described in the literature (Bonsall and Maradudin, 1977; Fujiki, De'Bell, and Geldart, 1987).

The basis of the summation technique is the separation of the interaction into a localized part and a long-range part. In the paper of Fujiki *et al.* (1987) this is accomplished by rewriting the dipolar energy given by Eq. (2) as

$$\mathcal{H}_{\rm dd}=-\frac{g}{2}\lim_{x\to 0}\sum_{i\neq j}\sigma_i^\alpha\sigma_j^\beta\frac{\partial}{\partial x_\alpha}\frac{\partial}{\partial x_\beta}\frac{1}{|\vec{r}_{ij}+\vec{x}|} \tag{6}$$

and making use of the identity

$$\frac{1}{r}=\frac{2}{\sqrt{\pi}}\int_0^\infty d\rho e^{-\rho^2r^2}$$

$$=\frac{2}{\sqrt{\pi}}\left(\int_0^\eta d\rho e^{-\rho^2r^2}+\int_\eta^\infty d\rho e^{-\rho^2r^2}\right), \tag{7}$$

where η is an arbitrary parameter typically of order unity. Substituting Eq. (7) into the expression for the dipolar sum given by Eq. (6) yields two terms, which we denote by $\mathcal{H}_1$ and $\mathcal{H}_2$, representing the contributions from integration over the intervals $\eta<\rho<\infty$ and $0<\rho<\eta$, respectively.

The second term in Eq. (7) may be evaluated explicitly as

$$\frac{2}{\sqrt{\pi}}\int_\eta^\infty d\rho e^{-\rho^2r^2}=\frac{\mathrm{erfc}(\eta r)}{r} \tag{8}$$

and hence $\mathcal{H}_1$ may be written as

$$\mathcal{H}_1=-\frac{g}{2}\sum_{i\neq j}\sigma_i^\alpha\sigma_j^\beta\gamma_1^{\alpha\beta}(\vec{r}_{ij}), \tag{9}$$

with $\gamma_1^{\alpha\beta}(\vec{r}_{ij})$ given by

$$\gamma_1^{\alpha\beta}(\vec{r}_{ij})=\lim_{x\to 0}\frac{\partial}{\partial x_\alpha}\frac{\partial}{\partial x_\beta}\left(\frac{\mathrm{erfc}(|\vec{r}_{ij}+\vec{x}|\,\eta)}{|\vec{r}_{ij}+\vec{x}|}\right). \tag{10}$$

This term may be readily evaluated numerically for different spin configurations since the complimentary error function $\mathrm{erfc}(x)$ damps exponentially for large x:

$$\lim_{x\to\infty} \mathrm{erfc}(x) \approx \frac{1}{\sqrt{\pi}} \frac{e^{-x^2}}{x}. \tag{11}$$

The term $\mathcal{H}_1$ therefore represents the contribution of the "short-range" part of the dipolar interaction to the energy of a particular spin configuration.

The remaining contribution to the dipolar contribution can be made rapidly convergent by transforming the expression for the dipolar energy to momentum ($\vec{q}$) space. The resultant expression may be written as

$$\mathcal{H}_2 = \frac{g}{2} \sum_{\vec{q}} \gamma_2^{\alpha\beta}(\vec{q}) \sigma_\alpha(\vec{q}) \sigma_\beta(-\vec{q}), \tag{12}$$

where $\sigma_\alpha(\vec{q})$ denotes the Fourier transform of the spin configuration,

$$\sigma_\alpha(\vec{q}) = \frac{1}{\sqrt{N}} \sum_i \sigma_i^\alpha e^{i\vec{q}\cdot\vec{R}_i}, \tag{13}$$

and $\gamma_2^{\alpha\beta}(\vec{q})$ may be calculated in a case of a rectangular lattice to give

$$\begin{aligned}\gamma_2^{\alpha\beta}(\vec{q}) = &-\frac{4}{3}\frac{\eta^3}{\sqrt{\pi}}\left(\delta_{\alpha\beta} - z_\alpha z_\beta \frac{3\pi}{\eta^2} \sum_{\vec{K}} e^{|\vec{q}-\vec{K}|^2/4\eta^2}\right) \\ &- 2\pi \sum_{\vec{K}} \left(z_\alpha z_\beta |\vec{q}-\vec{K}| - \frac{(q^\alpha - K^\alpha)(q^\beta - K^\beta)}{|\vec{q}-\vec{K}|}\right) \\ &\times \mathrm{erfc}\left(\frac{|\vec{q}-\vec{K}|}{2\eta}\right),\end{aligned} \tag{14}$$

where $\{\vec{K}\}$ denotes the reciprocal-lattice vectors of the rectangular lattice and z_α denotes the α component of the unit vector perpendicular to the surface. While the presence of the complimentary error function in the summation ensures a rapid convergence for large values of q, particular care has to be taken with the long-wavelength limit, since the first term in the series contains a nonanalytic contribution that goes as $q^\alpha q^\beta / q$. This contribution arises as a consequence of the long-range character of the dipolar interaction and often has to be treated separately. The nonanalytic character of this term can manifest itself in a number of interesting and subtle ways.

The summation technique described above, or some variant of it, provides a systematic way of rendering the dipolar sum rapidly convergent and a means of explicitly extracting the effect of the long-range character of the dipolar interaction. Generalizations of the above technique for simple antiferromagnetic structures were given by De'Bell and Whitehead (1991) and for striped phases by MacIsaac *et al.* (1995).

Finally, we note the almost trivial fact that the choice of η in the evaluation of $\mathcal{H}_1$ and $\mathcal{H}_2$ is quite arbitrary. However, the particular choice of η can affect the computational efficiency. Moreover, the fact that the individual values of $\mathcal{H}_1$ and $\mathcal{H}_2$ depend on the specific choice of η, while the sum is independent, provides a very important test of any algorithms used in the calculation of the dipolar energy.

B. Ground-state spin configurations

One important application of the Ewald summation technique is the determination of the dipolar contribution to the ground-state spin configuration. It can often happen that the contribution of the dipolar interaction will give rise to a finite energy difference between otherwise degenerate or nearly degenerate spin configurations. Therefore, despite its relatively small magnitude, the dipolar interaction can play an important role in determining the ground-state spin configuration.

In Table II we give the dipolar contribution to several important spin configurations. While this table by no means exhausts all of the possible spin configurations, it does include many of the experimentally important ones.

C. Dipole interaction and Monte Carlo simulations

Monte Carlo simulations are an important technique in the study of the finite-temperature properties of magnetic spin systems. We do not intend to cover the basis of the Monte Carlo procedure; instead we refer the reader to one of the many excellent texts on this subject (Binder and Heermann, 1993). In this section we wish to review some of the subtleties that can arise when the dipolar interaction is included in the simulation.

There are two ways in which the dipolar interaction affects the Monte Carlo procedure. The most obvious complication arises as a consequence of the fact that the dipolar interaction is not a simple nearest-neighbor interaction. Indeed, flipping a spin affects every other spin in the system. This means that many of the procedures that have been developed to improve the efficiency of the algorithm used in the Monte Carlo simulation, that either implicitly or explicitly exploit the finite range of the interaction, either have to be modified or are no longer applicable. It also means that the time required to perform a Monte Carlo step for an $L\times L$ site system increases as L^4, rather than L^2 for a localized interaction. This makes the problem extremely computation intensive and limits the size of the system that can be investigated in practice.

The other difficulty associated with including the dipolar interaction in a Monte Carlo simulation is how best to mitigate finite-size effects. Again, the long-range character of the dipolar interaction considerably complicates matters, as edge effects can give rise to an effective current loop around the boundary of the system if finite-size effects are not treated carefully.

A widely used method of modeling an infinite system by a finite number of degrees of freedom exploits the Ewald summation technique discussed in the previous section. The technique restricts the sum over states to those which are periodic. In the case of a square lattice, the only spin configurations included in the summation are those that satisfy the requirement

$$\sigma_\alpha(x,y) = \sigma_\alpha(x + n\times L, y + m\times L), \tag{15}$$

TABLE II. The dipolar energy calculated for a number of important spin configurations on a square lattice. The subscripts x and y refer to the square lattice axes; z is the perpendicular direction. Energies are expressed in units of $2a^3K_BT/\mu_{\rm eff}$. The function $f_h(i)$ is defined to be $f_h(i)\equiv(i-\mathrm{mod}(i,h))/h$.

System	Spin configuration	Energy
Planar ferromagnet	$\sigma_x=1$ $\sigma_y=0$ $\sigma_z=0$	$E=-4.5168g$
Planar antiferromagnet (AA) phase	$\sigma_x=(-1)^{i+j}$ $\sigma_y=0$ $\sigma_z=0$	$E=1.3229g$
Planar antiferromagnet (AF) phase	$\sigma_x=(-1)^{i}$ $\sigma_y=0$ $\sigma_z=0$	$E=-5.0989g$
Uniaxial ferromagnet	$\sigma_x=0$ $\sigma_y=0$ $\sigma_z=1$	$E=9.0336g$
Uniaxial antiferromagnet (AA) phase	$\sigma_x=0$ $\sigma_y=0$ $\sigma_z=(-1)^{i+j}$	$E=-2.6459g$
Uniaxial antiferromagnet (AF) phase	$\sigma_x=0$ $\sigma_y=0$ $\sigma_z=(-1)^{i}$	$E=-0.9355g$
Uniaxial striped phase	$\sigma_x=0$ $\sigma_y=0$ $\sigma_z=-1^{f_h(i)}$	$\lim_{h\to\infty}E_h=9.0336g-\frac{1}{h}(Ag+Bg\ln(h))$ $A=9.105,\ B=8$
Uniaxial checkerboard phase	$\sigma_x=0$ $\sigma_y=0$ $\sigma_z=-1^{f_h(i)+f_h(j)}$	$\lim_{h\to\infty}E_h=9.0336g-\frac{1}{h}(Ag+Bg\ln(h))$ $A=2.819,\ B=16$

where n and m are integers and where the x and y axes are within the square lattice and the z axis is perpendicular to it.

Such configurations may be completely specified in terms of L^2 spins in an $L\times L$ unit cell. Denoting by $\{\vec{R}_n\}$ the L^2 sites in the $L\times L$ unit cell and defining the lattice translation vector $\vec{T}$ as

$$\vec{T}=L(n\hat{x}+m\hat{y}), \tag{16}$$

where n and m are integers, one may write the dipolar energy as

$$\begin{aligned}\mathcal{H}_{\rm dip}&=\frac{g}{2}\sum_{i\neq j}\sigma_\alpha(\vec{r}_i)\sigma_\beta(\vec{r}_j)\gamma^{\alpha\beta}(\vec{r}_{ij})\\&=\frac{g}{2}\frac{N}{L^2}\sum_{i\neq j}^{L^2}\sigma_\alpha(\vec{R}_i)\Gamma^{\alpha\beta}(\vec{R}_{ij})\sigma_\beta(\vec{R}_j)\\&\quad+\frac{g}{2}NL^2\sum_{\vec{T}\neq 0}\gamma^{\alpha\alpha}(\vec{T}),\end{aligned} \tag{17}$$

where we have defined $\Gamma^{\alpha\beta}(\vec{R}_{ij})$ as

$$\Gamma^{\alpha\beta}(\vec{R}_{ij})=\sum_{\vec{T}}\gamma^{\alpha\beta}(\vec{R}_{ij}+\vec{T}). \tag{18}$$

Thus the calculation of the dipolar energy can be written as a sum over the L^2 spins that make up the $L\times L$ unit cell, which interact through an effective interaction $\Gamma^{\alpha\beta}(\vec{R}_{ij})$.

The evaluation of $\Gamma^{\alpha\beta}(\vec{R})$ is a straightforward but tricky business, particularly for large lattices. The Ewald summation techniques described in the previous section for performing dipolar sums are essential if reliable results are to be obtained.

We close this section by noting two points with regard to finite-size systems. The first point is that, while larger values of L generally lead to more reliable results, care has to be taken to ensure that the ground state is included in the subset of allowed spin configurations used in the analysis or, equivalently, that the ground state is commensurate with the imposed periodicity L. The second point is that the effective interaction can be used to calculate the dipolar energy of any spin configuration with a commensurate periodicity.

IV. SPIN WAVES

For a system whose spin dynamics are invariant under a continuous global rotation of the spins, the existence of long-range magnetic order implies the existence of a gapless branch in the spin-wave excitation spectrum. In the case of a localized interaction in two dimensions, such excitations lead to a divergence in the spin-wave (rms) amplitude at finite temperature which destroys the long-range magnetic order. For this reason, the exchange interaction is not sufficient to establish long-range magnetic order at finite temperature in two di-

mensions, a fact first realized by Bloch (1928) and later proved rigorously by Mermin and Wagner (1996).

The existence of long-range magnetic order in two-dimensional magnetic systems arises as a consequence of the magnetic surface anisotropy and the dipolar interaction. These interactions break the rotational invariance of the exchange interaction and, in the case of the dipolar interaction, introduce long-range interactions into the dynamics. This modifies the spin-wave spectra, rendering the fluctuations finite and stabilizing the long-range magnetic order.

To leading order the effect of fluctuations can be included by means of linearized spin-wave theory. Although linearized spin-wave theory is generally valid only at low temperatures, it can often provide important theoretical evidence for the existence of long-range magnetic order, together with a description of the low-temperature properties of the magnetically ordered state. In addition, spin-wave theory can be generalized to include higher-order corrections using modern techniques of many-body theory, which can be employed with some justification in the calculation of the critical temperature and the analysis of critical properties of these systems.

Spin-wave calculations come in one of two flavors, classical and quantum. In the classical case the spins are typically treated as vectors of fixed magnitude, which, following the usual convention, we denote by S. In the quantum-mechanical case the noncommutative algebra of the spin operators is taken into account. The analysis of classical spin systems can provide a qualitative description of many important features of a complicated magnetic system. Typically, the analysis of a classical spin system is far simpler than its quantum counterpart and, particularly in combination with the use of Monte Carlo methods, is used extensively in examining complex many-body effects. That said, however, a quantitative description of a magnetic system, particularly at low temperature, must include the quantum-mechanical nature of the spins. Spin-wave theory provides a useful bridge between the two approaches.

In this section we consider first a set of classical spins on a square lattice with a ferromagnetic exchange interaction and show how this case can be treated in the linearized spin-wave approximation. In particular we shall show how the long-range character of the dipolar interaction can play an essential role in determining the long-wavelength limit of the spin-wave spectra. We show how this can be generalized to a quantum mechanical spin-wave theory and present some results reported in the recent literature. We then extend the analysis to consider antiferromagnetic systems in the linearized spin-wave approximation. We close by discussing some work that goes beyond the linearized spin-wave theory.

In analyzing the properties of two-dimensional spin systems, one cannot neglect the dipolar interaction. Including the dipolar interaction considerably complicates the analysis of the spin-wave spectra.

A. Ferromagnetic case

In the absence of any magnetocrystalline anisotropy the energy may be written as

$$\mathcal{H}=\mathcal{H}_{\rm ex}+\mathcal{H}_{\rm dd} = -\frac{1}{2}\sum_{i\neq j}\left(J(\vec{R}_{ij})\vec{\sigma}_i\cdot\vec{\sigma}_j-\sum_{\alpha\beta}\gamma^{\alpha\beta}(\vec{R}_{ij})\sigma_i^\alpha\sigma_j^\beta\right), \quad (19)$$

where $\Sigma_{\alpha\beta}\gamma^{\alpha\beta}(\vec{R}_{ij})\sigma_i^\alpha\sigma_j^\beta$ denotes the dipolar interaction energy given by Eq. (2). If the exchange interaction is ferromagnetic in character and sufficiently strong to overcome the antiferromagnetic dipolar interaction, the ground state for the classical spin system will be ferromagnetic. From Table II we see that the dipolar interaction will favor the planar ferromagnetic ground state over the uniaxial ferromagnetic state.

To investigate the fluctuations about the ground-state spin configuration, we describe the components of the spin vector at the ith lattice site in terms of the angles θ_i and ϕ_i defined with respect to the magnetization axis, which we take as the z axis. We write

$$\sigma_i^1=S\sin(2\theta_i)\cos(\phi_i)=\frac{1}{2}(a_i+a_i^*)\sqrt{2S-a_i^*a_i}, \quad (20)$$

$$\sigma_i^2=S\sin(2\theta_i)\sin(\phi_i)=\frac{1}{2i}(a_i-a_i^*)\sqrt{2S-a_i^*a_i}, \quad (21)$$

and

$$\sigma_i^3=S\cos(2\theta_i)=S-a_i^*a_i, \quad (22)$$

where the complex amplitudes a_i are defined as

$$a_i=\sqrt{2S}\sin(\theta_i)e^{i\phi_i}. \quad (23)$$

The amplitudes a_i and their complex conjugates a_i^* are the classical analogs of the quantum-mechanical creation and annihilation operators in the Holstein-Primakoff representation of quantum spins (Holstein and Primakoff, 1940).

Assuming the fluctuations are small, one can expand the Hamiltonian given by Eq. (19) to second order in the spin-wave amplitudes to give

$$H=E_0+\frac{1}{2}\sum_{\vec{q}}\Psi^\dagger(\vec{q})\Sigma(\vec{q})\Psi(\vec{q}) \quad (24)$$

with

$$\Psi(\vec{q})=\begin{pmatrix}a(\vec{q})\\ a^*(-\vec{q})\end{pmatrix}, \quad (25)$$

and

$$\Sigma(\vec{q})=\begin{pmatrix}\Omega(\vec{q}) & \Delta(\vec{q})\\ \Delta(\vec{q}) & \Omega(\vec{q})\end{pmatrix}, \quad (26)$$

where the matrix elements $\Omega(\vec{q})$ and $\Delta(\vec{q})$ are defined as

$$\Omega(\vec{q})=S\left(-J(\vec{q})+J(0)+\frac{1}{2}(\gamma_{11}(\vec{q})+\gamma_{22}(\vec{q}))-\gamma_{33}(0)\right), \quad (27)$$

and

$$\Delta(\vec{q}) = \frac{S}{2}(\gamma_{11}(\vec{q}) - \gamma_{22}(\vec{q})). \tag{28}$$

To evaluate the spin-wave contribution to the free energy and the magnetization, the Hamiltonian is diagonalized using a technique described by White, Sparks, and Ortenburger (1965). This requires that we obtain the transformation matrix $S(\vec{q})$ that diagonalized the Hamiltonian, to give

$$S^{\dagger}(\vec{q})\Sigma(\vec{q})S(\vec{q}) = \Lambda(\vec{q}) \tag{29}$$

where $\Lambda(\vec{q})$ denotes the diagonal eigenvalue matrix.

The eigenvalue problem defined by Eq. (29) is complicated by the fact that the transformation matrix $S(\vec{q})$ is not unitary but instead satisfies the condition

$$S(\vec{q})gS^{\dagger}(\vec{q}) = g, \tag{30}$$

with

$$g = \begin{pmatrix} 1 & 0 \\ 0 & -1 \end{pmatrix}. \tag{31}$$

This condition ensures that the phase-space integral is left invariant under the transformation defined by the matrix S.

In the case of a ferromagnetic order parameter, we readily obtain

$$\Lambda(\vec{q}) = \begin{pmatrix} \varepsilon(\vec{q}) & 0 \\ 0 & \varepsilon(\vec{q}) \end{pmatrix} \tag{32}$$

with

$$\varepsilon(\vec{q}) = \sqrt{\Omega(\vec{q})^2 - \Delta(\vec{q})^2}, \tag{33}$$

while the transformation matrix $S(\vec{q})$ is given by

$$S(\vec{q}) = \begin{pmatrix} u(\vec{q}) & v(\vec{q}) \\ v(\vec{q}) & u(\vec{q}) \end{pmatrix}, \tag{34}$$

with

$$u(\vec{q}) = \sqrt{\frac{\Omega(\vec{q}) + \varepsilon(\vec{q})}{2\varepsilon(\vec{q})}} \tag{35}$$

and

$$v(\vec{q}) = \sqrt{\frac{\Omega(\vec{q}) - \varepsilon(\vec{q})}{\varepsilon(\vec{q})}}. \tag{36}$$

It is straightforward to show that this transformation reduces to the familiar Bogoliubov transformation, although the technique described by White *et al.* (1965) can be readily generalized to treat more complicated situations such as the antiferromagnetic case.

The interaction $\gamma_{\alpha\beta}(\vec{q})$ may be calculated using the techniques described in Sec. III.A to give, in the limit $q \to 0$,

$$\gamma_{11}(\vec{q}) = \gamma_{\perp}^{0} - g2\pi q + O(q^2), \tag{37}$$

$$\gamma_{22}(\vec{q}) = \gamma_{\parallel}^{0} + g2\pi\frac{q_2^2}{q} + O(q^2), \tag{38}$$

$$\gamma_{33}(\vec{q}) = \gamma_{\parallel}^{0} + g2\pi\frac{q_3^2}{q} + O(q^2). \tag{39}$$

Here

$$\gamma_{\perp}^{0} = g\sum_{\vec{R}\neq 0}\frac{1}{R^3} \equiv g\frac{8\pi\alpha}{3} \tag{40}$$

$$\gamma_{\parallel}^{0} = g\sum_{\vec{R}\neq 0}\left(\frac{1}{R^3} - 3\frac{y^2}{R^5}\right) = -g\frac{4\pi\alpha}{3}, \tag{41}$$

where α may be calculated for the square lattice to give $\alpha = 1.078$. Substituting these values into the expression for the $\Omega(\vec{q})$ and $\Delta(\vec{q})$, we obtain in the long-wavelength limit

$$\Omega(\vec{q}) = \frac{gS}{2}\left(4\pi\alpha - \frac{2\pi}{q}(q^2 - q_y^2)\right) + JSq^2 \tag{42}$$

$$\Delta(\vec{q}) = \frac{gS}{2}\left(4\pi\alpha - \frac{2\pi}{q}(q^2 + q_y^2)\right), \tag{43}$$

where we have assumed a nearest-neighbor exchange interaction. This yields the following expression for the spin-wave energy in the long-wavelength limit:

$$\lim_{q\to 0}\varepsilon(\vec{q}) = 2\pi gS|\sin\theta_{\vec{q}}|\sqrt{2\alpha q} + \cdots. \tag{44}$$

Thus, while the spin-wave spectra remain gapless, we see that the energy varies as $\sqrt{q}$ in the long-wavelength limit, a result first obtained by Male'ev (1976). This result shows how the long-range nature of the dipolar interaction manifests itself in the low-energy excitations of the system.

The free energy in the linearized spin-wave approximation may be easily evaluated to give

$$F = E_0 - k_B T\sum_{\vec{q}} \ln\frac{\pi k_B T}{\varepsilon(\vec{q})} \tag{45}$$

together with the magnetization, which is given by

$$m = S\left(1 - \frac{2}{N}\sum_{\vec{q}}\langle a^*(\vec{q})a(\vec{q})\rangle\right)$$

$$= S - k_B T\frac{2S}{N}\sum_{\vec{q}}\frac{\Omega(\vec{q})}{\varepsilon(\vec{q})^2}. \tag{46}$$

It is readily seen that the summand in Eq. (46) diverges as $1/q$ in the long-wavelength limit and hence the summation will be well defined in the limit $N \to \infty$. This is quite different from the case of a pure ferromagnetic exchange model in which the spin-wave contribution to the magnetic order parameter diverges as $\ln N$ in the limit that $N \to \infty$. The fact that the summation in Eq. (46) is finite in the limit $N \to \infty$ implies that, unlike the isotropic exchange interaction case, the long-range molecular order persists to finite temperature. This result, first obtained by Male'ev (1976), demonstrates the importance of the modification to the spectra that arises from a subtle combination of anisotropic and long-range characteristics in the dipolar interaction.

The classical spin-wave theory described above can be readily generalized to the case of a quantum spin system

in which the spin variables are operators which satisfy the angular momentum algebra

$$[\hat{\sigma}_i^\alpha, \hat{\sigma}_j^\beta] = \epsilon_{\alpha\beta\gamma}\hat{\sigma}_i^\gamma \delta_{ij} \tag{47}$$

with

$$\sum_\alpha \hat{\sigma}_i^\alpha \hat{\sigma}_i^\alpha = S(S+1). \tag{48}$$

The expression for the spin operators given by Eqs. (20), (21), and (22) is still valid, provided the complex coefficients are replaced by the operators $\hat{a}_i$ and $\hat{a}_i^\dagger$, which satisfy the familiar Bose-Einstein commutation relations, and the proper ordering is used.

The free energy is given in the quantum-mechanical case as

$$F = \tilde{E}_0 - k_B T \sum_{\vec{q}} \ln(e^{\varepsilon(\vec{q})/k_B T} - 1), \tag{49}$$

while the magnetization may be calculated in the linearized spin-wave approximation as

$$m = \tilde{m}_0 - \frac{2S}{N} \sum_{\vec{q}} \frac{\Omega(\vec{q})}{\varepsilon(\vec{q})} \frac{1}{e^{\varepsilon(\vec{q})/k_B T} - 1}. \tag{50}$$

The zero-temperature order parameter $\tilde{m}_0$ is reduced from the classical value of S due to the noncommutative nature of the spin-wave operators, which represent the reduction in the magnetic moment owing to quantum-mechanical fluctuations of the spins in the ground state.

Male'ev (1976) calculated the temperature dependence of the magnetization in the case of the quantum-mechanical spins for low and high temperatures. He obtained the following result:

$$1 - \frac{m(T)}{m_0} = \begin{cases} \dfrac{\Gamma\left(\frac{3}{4}\right)\xi\left(\frac{3}{2}\right)}{\Gamma\left(\frac{5}{4}\right)} \left(\dfrac{\alpha^2}{2\pi S}\right)\left(\dfrac{k_B T}{4\pi\alpha g S}\right)^{3/2}\left(\dfrac{J\alpha}{g\pi}\right)^{1/4} & k_B T \ll 4\pi\alpha g S\sqrt{\dfrac{g\pi}{2J\alpha}} \\ \dfrac{1}{4\pi S}\left(\dfrac{k_B T}{JS}\right)\ln\left(\dfrac{k_B T}{\pi S g}\sqrt{\dfrac{J}{g\pi\alpha}}\right) & k_B T \gg 4\pi\alpha g S\sqrt{\dfrac{g\pi}{2J\alpha}}. \end{cases} \tag{51}$$

Yafet, Kwo, and Gyorgy (1986) arrived at a result similar to Male'ev's (1976); however, they evaluated the integral given by Eq. (50) in the limit $N \to \infty$ by separating the low-energy part, which they treated classically, and the high-energy part, which they evaluated by neglecting the anisotropy induced by the dipolar interaction. As a consequence of their approximation their results differ from Male'ev's (1976) at low temperature, showing a linear dependence of the magnetization on temperature in the limit $T \to 0$. Yafet *et al.* (1986) did extend their results to consider multilayer domains and examine the transition to bulk behavior with increasing layer thickness.

In the absence of the dipolar interaction, it has been shown by a number of authors (e.g., Herring and Kittel, 1951; Döring, 1961a, 1961b; Corciovei, 1963) that the presence of a uniaxial anisotropy can introduce a gap in the spin-wave spectrum at $q = 0$ and hence render the fluctuations finite. This results in finite long-range molecular ordering at finite temperature.

The combined effect of a finite anisotropy and a dipolar interaction in a ferromagnetic thin film has been studied in the spin-wave approximation by a number of author (Bruno, 1991; Erickson and Mills, 1992). In the analysis by Bruno (1991) the following form for the surface anisotropy is used:

$$H_\kappa = -\kappa \sum_{\langle ij \rangle} (\vec{\sigma}_i \cdot \vec{\sigma}_j - 3(\vec{\sigma}_i \cdot \vec{u}_{ij})(\vec{\sigma}_j \cdot \vec{u}_{ij})), \tag{52}$$

where the sum $\langle ij \rangle$ is over nearest-neighbor pairs and $\vec{u}_{ij}$ denotes the unit vector connecting the pair $\langle ij \rangle$. This form of the anisotropy has the advantage that it automatically matches the symmetry of the underlying lattice.

Bruno (1991) takes the difference between the dipolar energy for perpendicular magnetization and that for parallel magnetization and combines this with the surface anisotropy term to define an effective anisotropy coefficient κ_{eff} given by

$$\kappa_{\text{eff}} = \kappa - g\frac{2\pi\alpha}{3}. \tag{53}$$

For $\kappa_{\text{eff}} > 0$, the easy axis of magnetization is perpendicular to the plane of the film. In this case, the linear spin-wave theory yields an expression for the energy of the form given by Eq. (24) for a planar ferromagnet; however, the coefficients $\Omega(\vec{q})$ and $\Delta(\vec{q})$ are given in the long-wavelength limit by

$$\Omega(\vec{q}) = 6S\kappa_{\text{eff}} + gS\pi q + JSq^2 \tag{54}$$

$$\Delta(\vec{q}) = gS\pi q, \tag{55}$$

which yields the following expression for the spin-wave spectra in the limit $q \to 0$ (Bruno, 1991):

$$\epsilon(\vec{q}) = 6S\kappa_{\rm eff} + JSq^2. \tag{56}$$

Note that the effect of the anisotropy is to induce a gap in the spin-wave spectra and that the effect of the dipolar interaction is included in $\kappa_{\rm eff}$. The temperature dependence of the magnetization can be calculated using Eq. (50) to give

$$1 - \frac{m(T)}{m_0} = -\frac{1}{4\pi S}\left(\frac{k_B T}{JS}\right)\ln(1 - e^{-6\kappa_{\rm eff} S/k_B T}) \tag{57}$$

$$= \begin{cases} \dfrac{1}{4\pi S}\left(\dfrac{k_B T}{JS}\right) e^{-6\kappa_{\rm eff} S/k_B T} & k_B T \ll 6S\kappa_{\rm eff} \\ \dfrac{1}{4\pi S}\left(\dfrac{k_B T}{JS}\right)\ln\left(\dfrac{k_B T}{6S\kappa_{\rm eff}}\right) & k_B T \gg 6S\kappa_{\rm eff}. \end{cases} \tag{58}$$

The presence of the gap induced by the surface anisotropy renders the rms spin-wave amplitude finite and hence leads to finite long-range molecular ordering at finite temperature.

One obvious difficulty with the above analysis is that the ground state for a dipolar system with a ferromagnet exchange interaction, in which the easy axis is perpendicular to the plane, is not the homogeneous ferromagnetic phase assumed in the above analysis but is instead the striped phase (Garel and Doniach, 1982; Yafet and Gyorgy, 1988; Kaplan and Gehring, 1993; Taylor and Gyorffy, 1993; MacIsaac *et al.*, 1995).

Because of the particular form chosen for the surface anisotropy, the analysis for the easy-plane easy axis ($\kappa_{\rm eff} < 0$) is then identical to that presented previously for the ferromagnetic dipolar state except that the expressions for $\Omega(\vec{q})$ and $\Delta(\vec{q})$, given by Eqs. (42) and (43), are modified to yield in the long-wavelength limit

$$\Omega(\vec{q}) = 3S|\kappa_{\rm eff}| - g\frac{\pi S}{q}(q^2 - q_y^2) + JSq^2 \tag{59}$$

and

$$\Delta(\vec{q}) = 3S|\kappa_{\rm eff}| - g\frac{\pi S}{q}(q^2 + q_y^2). \tag{60}$$

In his analysis, Bruno (1991) shows that for $0 < |\kappa_{\rm eff}| < \kappa_c$ ($\kappa_c = \pi^2 g^2/6J$) the stability criterion for the spin-wave eigenvalue spectrum, $\Omega(\vec{q}) > |\Delta(\vec{q})|$, is not satisfied for all values of $\vec{q}$. Specifically, Bruno (1991) shows that for this range of κ the above spectrum exhibits a soft mode at $q = q_c$ ($q_c = \pi g/J$) with

$$\varepsilon(\vec{q}_c) = 0 \tag{61}$$

and that the above spectrum is negative in the vicinity of $q = q_c$. This implies that the homogeneous planar phase is unstable against the formation of a spatially modulated phase with a wavelength of the order of $q \approx q_c$. While the existence of such a phase would be of obvious interest from an experimental viewpoint, Bruno (1991) suggests that the narrow range of κ required for the existence of an oscillatory phase makes it unlikely that it would be observed. A similar instability is discussed in the later work of Erickson and Mills (1992) for the case of an applied external field H oriented parallel to the plane. In the case of a uniaxial anisotropy ($\kappa_{\rm eff} > 0$) it is shown that if H is sufficiently large to overcome the effect of the anisotropy, such that the spins are forced to lie in the plane, then there exists a range $H_c^- < H < H_c^+$, with

$$2\mu_B H_c^{\pm} = S\left(6\kappa_{\rm eff} \pm \frac{\pi^2 g^2}{J}\right), \tag{62}$$

in which the ferromagnetic state is unstable against the formation of a spatially inhomogeneous phase. Erickson and Mills (1992) suggest that the domain structure in this phase is similar to that discussed by Yafet and Gyorgy (1988) and others, although the nature of the relationship is not made explicit. This result has some interesting implications when generalized to include finite-temperature corrections to the anisotropy and exchange constant.

If the anisotropy is such that $\kappa_{\rm eff} < -\kappa_c$, then the energy spectrum is real and the spin-wave spectrum can be obtained from a straightforward modification of Eq. (44) to yield the following expression for the spin-wave energy:

$$\varepsilon(\vec{q}) = 2S\sqrt{3\pi g|\kappa_{\rm eff}|q}\,|\sin\theta_{\vec{q}}| + JSq^2 + \cdots \tag{63}$$

in the long-wavelength limit. Averaging out the angular dependence of $\epsilon(\vec{q})$, Bruno (1991) obtains the following expressions for the magnetization in the low-temperature and high-temperature limits:

$$1 - \frac{m(T)}{m_0} = \begin{cases} \dfrac{\zeta(3)}{4S}\dfrac{(k_B T)^3}{(\pi S g)^2 6|\kappa_{\rm eff}|S} & k_B T \ll 6S\kappa_{\rm eff} \\ \left(\dfrac{k_B T}{4\pi JS^2}\right)\ln\left(\dfrac{2k_B T}{\pi S g}\sqrt{\dfrac{J}{6|\kappa_{\rm eff}|}}\right) & k_B T \gg 6S\kappa_{\rm eff}. \end{cases} \tag{64}$$

It should be noted that the low-temperature result given above differs somewhat from that given by Male'ev (1976) in Eq. (51). This difference may be attributed to the approximate treatment of the planar anisotropy of the spin-wave energy by Bruno (1991).

The high-temperature limit is also interesting in that it is of exactly the same form as the corresponding result for the perpendicular easy axis, even although the spin-wave spectrum is gapless. This equivalence can be made quantitative by introducing a pseudogap,

$$\epsilon_{\rm pg}=\frac{\pi S g}{2}\sqrt{\frac{6|\kappa_{\rm eff}|}{J}}. \tag{65}$$

B. Antiferromagnetic interaction ($J<0$)

The role of the dipolar interaction in stabilizing long-range molecular order also extends to the case of antiferromagnetic exchange, although the mechanism is somewhat different. In the absence of a dipolar interaction, the two-dimensional Heisenberg model with an antiferromagnetic exchange constant ($J<0$) is invariant under a global rotation of the spins and hence will not exhibit any long-range molecular ordering. The antiferromagnetic nature of the Goldstone modes means that the long-range character of the dipolar interaction will not qualitatively modify the excitation spectrum at long wavelengths. However, the dipolar interaction will break spin rotational invariance and remove the degeneracy between the magnetic ground states, thus introducing a gap in the spin-wave spectrum. This will render the magnetic fluctuations finite and stabilize long-range molecular order at finite temperature.

If the exchange interaction is antiferromagnetic in character then it is reasonable to suppose that, if the magnitude of the interaction were sufficiently large, the ground-state spin configuration would switch from the dipolar ground state to an antiferromagnetic configuration in which each spin would be aligned antiparallel to each of its nearest neighbors. From the results presented in Table II it is clear that (in the absence of other anisotropies) the dipolar interaction would favor the planar antiferromagnetic (AF) phase over the uniaxial, perpendicular antiferromagnetic (AA) phase. If we assume a nearest neighbor exchange interaction, then the stability of the perpendicular antiferromagnetic (AA) phase requires that the exchange constant satisfy the condition $|J|>(5.0989-2.6459)g/2=1.2265g$.

To analyze the antiferromagnetic dipolar system, one splits the lattice into a and b sublattices in which the nearest neighbors of each site on the a sublattice belong to the b sublattice and vice versa. Denoting the spins on the a and b sublattices by σ_i^a and σ_i^b, respectively, one can write the spin vectors in terms of the complex amplitudes a_i and b_i as

$$\sigma_i^{1a}=\frac{1}{2}(a_i+a_i^*)\sqrt{2S-a_i^*a_i} \tag{66}$$

$$\sigma_i^{2a}=\frac{1}{2i}(a_i-a_i^*)\sqrt{2S-a_i^*a_i} \tag{67}$$

$$\sigma_i^{3a}=S-a_i^*a_i \tag{68}$$

and

$$\sigma_i^{1b}=\frac{1}{2}(b_i+b_i^*)\sqrt{2S-b_i^*b_i} \tag{69}$$

$$\sigma_i^{2b}=-\frac{1}{2i}(b_i-b_i^*)\sqrt{2S-b_i^*b_i} \tag{70}$$

$$\sigma_i^{3b}=-S+b_i^*b_i\,. \tag{71}$$

The presence of the dipolar interaction considerably complicates the spin-wave Hamiltonian for the antiferromagnetic ground state; not only do we have quadratic terms of the form $a(\vec{q})a(-\vec{q})$ and $b(\vec{q})b(-\vec{q})$, but there are also terms coupling the amplitudes associated with the fluctuations on each of the two sublattices. Therefore, while the spin-wave Hamiltonian is of the same form as Eq. (24), the matrix $\Sigma(\vec{q})$ is a 4×4 matrix, coupling together the various amplitudes for the a and b sublattices.

Despite the increased complexity, the spin-wave Hamiltonian can be diagonalized using the method of White *et al.* (1965) described earlier for the ferromagnetic case, and the spin-wave spectrum may be determined from the solution of an eigenvalue equation analogous to that given in Eq. (29) for the ferromagnetic case.

In contrast to the simple nearest-neighbor exchange model, the excitation spectrum is no longer degenerate but instead splits into two branches. Pich and Schwabl (1993) have analyzed the antiferromagnetic dipolar spin system on a square lattice in considerable detail for the case $|J|\gg g$. They show that, for realistic ratios $g/|J|\approx10^{-3}$, the splitting between the two branches is negligible. Therefore, for sufficiently large values of $|J|$, the two branches are essentially degenerate and the spectrum is given in the long-wavelength limit by

$$\lim_{q\to0}\varepsilon_{\pm}(\vec{q})=4S\sqrt{\varepsilon_0^2+2J^2q^2} \tag{72}$$

with ε_0 given by

$$\varepsilon_0=\sqrt{|J|((\gamma_\perp^a-\gamma_\parallel^a)-(\gamma_\perp^b-\gamma_\parallel^b))} \tag{73}$$

where

$$\gamma_\perp^a=\sum_{\vec{R}_a}\gamma^{33}(\vec{R}_a), \tag{74}$$

$$\gamma_\parallel^a=\sum_{\vec{R}_a}\gamma^{11}(\vec{R}_a)=\sum_{\vec{R}_a}\gamma^{22}(\vec{R}_a), \tag{75}$$

$$\gamma_\perp^b=\sum_{\vec{R}_b}\gamma^{33}(\vec{R}_b), \tag{76}$$

$$\gamma_\parallel^b=\sum_{\vec{R}_b}\gamma^{11}(\vec{R}_b)=\sum_{\vec{R}_b}\gamma^{22}(\vec{R}_b). \tag{77}$$

The dipolar interaction therefore induces a gap in the spin-wave spectrum in the limit $q\to0$, which is proportional to the geometric mean of the exchange and dipo-

lar interactions. This arises as a consequence of the difference between the dipolar energy for the in-plane and out-of-plane states and serves to stabilize the magnetic order at finite temperature.

Pich and Schwabl (1993) also obtain a simplified expression for the magnetization in the limit $g/|J| \ll 1$ and, using the long-wavelength limit for the excitation spectrum given by Eq. (72), they obtain the following estimate for the Néel temperature T_N:

$$T_N \approx \frac{8S|J|}{\ln\left(\frac{2|J|}{\varepsilon_0}\right)}. \tag{78}$$

This yields an estimated value of $T_N = 112$ K for the quasi-two-dimensional antiferromagnet K_2MnF_4, as compared to the measured value of 42 K. However, as we shall discuss in the next section, this discrepancy may be largely attributed to the simplified form of the spectrum used to obtain the above estimate of T_N.

While Pich and Schwabl (1993) considered the case $|J| \gg g$, Corruccini and White (1993) analyzed the pure dipolar spin system ($J=0$) on both a simple cubic lattice and a square lattice using linearized spin-wave theory. In the absence of the exchange interaction and magnetocrystalline anisotropy, in the ground state of the square lattice the spins lie in the plane and are aligned antiferromagnetically as shown in Fig. 3. The analysis is similar to that presented above and the spin-wave spectrum exhibits two nondegenerate branches, with a gapless mode that varies linearly with wave number q in the long-wavelength limit (Corruccini and White, 1993). From their spin-wave analysis, Corruccini and White conclude that the two-dimensional square dipolar lattice does not exhibit long-range magnetic order at finite temperature.

This conclusion of Corruccini and White (1993) regarding a square dipolar lattice appears to be contradicted by Monte Carlo simulations on a classical dipolar lattice (De'Bell *et al.*, 1997). While it is certainly problematic to demonstrate the existence of long-range magnetic order in two-dimensional spin systems by simulations on finite-size systems, some subtleties in the interpretation of linearized spin-wave theory are revealed by a study of a planar spin system (De'Bell *et al.*, 1997). In this analysis it is shown that, even though the dipolar interaction is not invariant under a global rotation of the spins, the ground-state energy is nevertheless degenerate. The ground-state spin configurations define a continuous manifold of states and the zero-energy mode corresponds to an infinitesimal displacement within this manifold. A similar result was shown for an analogous nearest-neighbor interaction (Henley, 1989; Prakash and Henley, 1990).

What distinguishes this situation from the case of a degeneracy arising from continuous symmetry is the fact that in the dipolar interaction the degeneracy is destroyed by coupling between modes with finite wave vector. The existence of a gapless mode is therefore an artifact of the linear spin-wave approximation, which neglects mode coupling. The effect of the coupling would be to induce a gap in the spin-wave mode at finite temperature and, in the case of quantum spins, in the ground state. Such effects can be incorporated, at least to leading order, by means of a renormalized spin-wave theory (Whitehead, 1996).

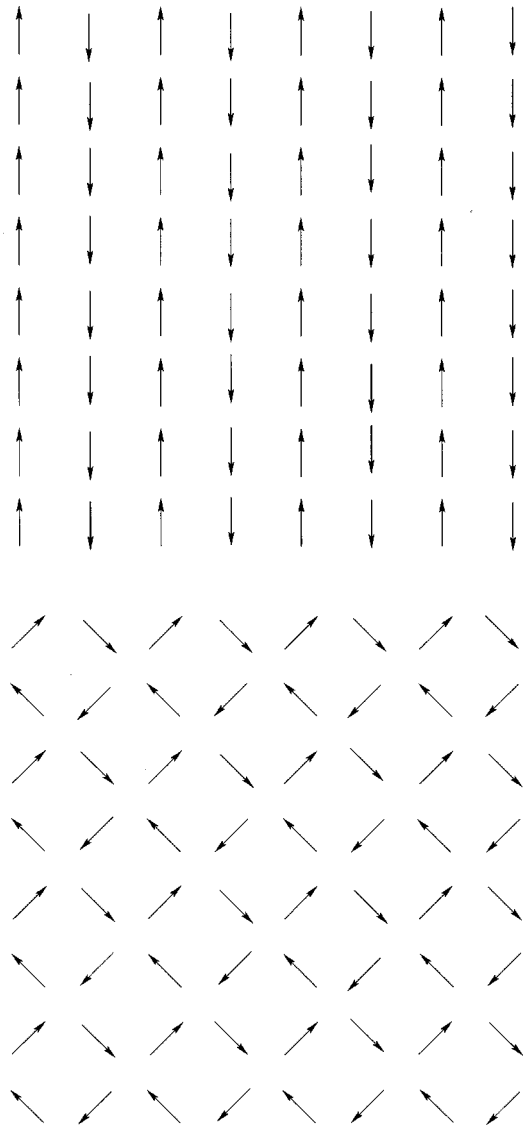

FIG. 3. Two degenerate antiferromagnetic ground states of a pure dipolar system. These two states belong to a continuum of ground states for this system (De'Bell *et al.*, 1997).

C. Corrections to linearized spin-wave theory

The previous discussion emphasizes the potential significance of higher-order terms in the expansion of the Hamiltonian, even at low temperature. Even when the linearized theory provides an adequate description of the low-temperature regime, incorporating higher-order corrections can extend the range of spin-wave theory to higher temperatures. Unfortunately, incorporating higher-order corrections in a systematic way that includes the important effects induced by the dipolar interaction in two-dimensional systems is difficult. There

are nevertheless a number of results that generalize aspects of the work described in the previous sections.

In the case of the ferromagnetic systems, De'Bell and Geldart (1989) have studied the critical exponents of two-dimensional dipolar magnetic systems by means of an ϵ expansion. Generalizing to d dimensions, the Hamiltonian for a system given by Male'ev (1976), De'Bell and Geldart (1989) find that the critical exponents of the phase transition will be determined by the same forms as the usual ϵ expansion, with $\epsilon=2$ in the case of two dimensions. However, they show that if the Hamiltonian is modified to consider uniaxial, rather than isotropic, ordering, then a new ϵ' expansion is required about an upper critical dimension $d_c=3\frac{1}{2}$. The authors suggest that the effects of the dipolar interaction may account for features observed close to the transition in Gd on W films (Baberschke, Farle, and Zomach, 1987; Farle and Baberschke, 1987).

Erickson and Mills (1992) have generalized their results (discussed above) to include higher-order effects, by means of a diagrammatic technique similar to that used in the analysis of superfluidity of a dilute Bose gas. In particular, they show that the spin-wave spectrum is of the same functional form as the linearized theory except that the effective anisotropy and the exchange are replaced by temperature-dependent parameters. In the case $\kappa_{\rm eff}>0$ and $H=0$, their results may be expressed as

$$1-\frac{\kappa_{\rm eff}(T)}{\kappa_{\rm eff}}\approx\frac{k_BT}{16\pi|J|S^2}\ln\left(\frac{k_BT}{6\kappa_{\rm eff}S}\right), \tag{79}$$

$$1-\frac{J(T)}{J}\approx\frac{1}{32\pi S}\left(\frac{k_BT}{4JS}\right)\zeta(2). \tag{80}$$

These results are qualitatively similar to the classical results obtained earlier by Pescia and Pokrovsky (1990); however, as Erickson and Mills (1992) point out, the classical treatment of Pescia and Pokrovsky (1990) substantially overestimates renormalization effects in these systems. [See also the comment by Levanyuk and Garcia (1993) and reply by Pescia and Pokrovsky (1993), and the comments by Chui (1995a).] These results provide an interesting interpretation of the reorientation transition observed by Pappas *et al.* (1990).

In the case of an antiferromagnetic system, Pich and Schwabl (1994) have generalized their linearized spin-wave theory to include higher-order effects using the method of Callen (1963). Within this approximation scheme, the spin-wave spectrum is of the same functional form as that obtained in the linearized theory except that the factor S is replaced by $m(T)$. This implies that the spin waves soften with increasing temperature. Generalizing their earlier analysis, Pich and Schwabl (1994) show that the approximate expression for the Néel temperature, given by Eq. (78) is modified to give

$$T_N\approx\frac{8S|J|}{\ln\left(\frac{2|J|}{\tilde{\varepsilon}_0}\right)}, \tag{81}$$

where $\tilde{\varepsilon}_0=(\tilde{m}_0/S)\varepsilon_0$ and $\tilde{m}_0$ denotes the zero-temperature magnetization, including the effect of quantum fluctuations. Pich and Schwabl (1994) also present numerical estimates of the Néel temperature calculated using full dispersion over the Brillioun zone and compare their theoretical results with the values obtained experimentally for several of the quasi-two-dimensional tetragonal antiferromagnetic halides, K_2MnF_4, Rb_2MnF_4, and $(CH_3NH_3)_2MnCl_4$. Given the assumptions used in the analysis, the agreement is very good.

V. ORDERED STATES AND PATTERN FORMATION

As described in Sec. II, ultrathin metal-on-metal magnetic films exhibit complex domain structures on mesoscopic scales and a number of transitions between magnetic states with different morphologies. By contrast, the layered rare-earth systems exhibit relatively simple antiferromagnetic structures, which can be defined in terms of unit cells on an interatomic length scale. In this section we summarize a number of theoretical results for both types of system and compare these with experiment.

A. Rare-earth systems

In Sec. II.B we discussed the observed magnetic properties of the rare-earth ions in the compounds $REBa_2Cu_3O_{7-\delta}$. In particular, it was shown that for the heavier compounds—RE=Nd, Sm, Er, Dy, and Gd—the presence of a magnetic sublattice had little effect on the superconducting properties. The observed nature of these compounds suggests that the magnetic properties of the rare-earth sublattice may be described in terms of a simple model that incorporates the short-ranged exchange interaction, the dipolar interaction, and an on-site crystalline electric field (CEF) anisotropy. Of these interactions, the dipolar interaction and the CEF can be specified with a considerable degree of precision, while the exchange interaction may be given in terms of a single parameter.

Early work by De'Bell and Whitehead (1991) showed that, despite the long-range character of the dipolar interaction, coupling between rare-earth ions on adjacent layers was negligibly small. This is consistent with the observation that the critical fluctuations in many of the compounds appear to be two dimensional in nature and that the ordering along the c axis is sensitive to the degree of oxygenation and the manner in which the sample is prepared. In the first instance, we may therefore regard these compounds as quasi two dimensional and consider coupling between adjacent layers separately.

Of the $REBa_2Cu_3O_{7-\delta}$ compounds the most extensively studied are the Dy, Gd, and Er compounds. Of these, it is most useful to consider first $DyBa_2Cu_3O_{7-\delta}$. Crystalline electric-field calculations by De'Bell and Whitehead (1994) show that the ground state of the Dy^{3+} is a Kramers doublet, with a highly anisotropic magnetic moment aligned along the c axis. This implies that $DyBa_2Cu_3O_{7-\delta}$ may be realistically modeled by a

uniaxial spin system (s=1/2) on a square lattice in which the spins interact through the dipolar interaction and an antiferromagnetic exchange interaction. The appropriate Hamiltonian can be written, using the notation of MacIsaac *et al.* (1992), as

$$\mathcal{H}=\frac{\mu_{\rm eff}^2}{2a^3}\left(\sum_{i\neq j}\frac{s_i s_j}{R_{ij}^3}-\mathcal{J}\sum_{\langle ij\rangle}s_i s_j\right), \tag{82}$$

where $s_i=\pm 1$.

It may be readily shown that the pure dipolar interaction ($\mathcal{J}=0$) yields the observed ground-state spin configuration. Monte Carlo simulations by MacIsaac *et al.* (1992) show that the Néel temperature for the pure dipolar case is given by

$$\frac{2a^3k_BT_n}{\mu_{\rm eff}^2}=2.39\pm 0.5. \tag{83}$$

Using a value of $\mu_{\rm eff}=7.25\mu_{\rm B}$ (Goldman *et al.*, 1987), however, yields a value $T_N=0.67$ K, significantly less than the measured value of 0.95 K, implying that the exchange interaction cannot be neglected and is of comparable strength to the dipolar interaction (Whitehead *et al.*, 1993). Extending their simulations to include the effects of the exchange interaction, MacIsaac *et al.* (1992) obtain the following relationship between the Néel temperature and the exchange constant $\mathcal{J}$:

$$\frac{2a^3k_BT_n}{\mu_{\rm eff}^2}=2.4242+2.3523|\mathcal{J}|. \tag{84}$$

Fitting the observed transition temperature to the interpolation formula of Eq. (84), MacIsaac *et al.* (1992) obtain a value for the exchange constant $\mathcal{J}=0.509$.

These simulations also show that, despite the long-range character of the dipolar interaction, the critical exponents of the uniaxial dipolar model are consistent with those of the two-dimensional Ising model.

In the case of $ErBa_2Cu_3O_{7-\delta}$, CEF calculations show that the ground state of the Er^{3+} ion is a Kramers doublet. For the orthorhombic phase, the calculation of the effective magnetic moment gives the *b* axis as the easy axis, although it should be noted that the effective magnetic moment has a significant component along both the *a* and *c* axes. Simulations on a uniaxial dipolar spin system ($J=0$) on a square lattice in which the spins are aligned along the *x* axis yields a Néel temperature

$$\frac{2a^3k_BT_n}{\mu_{\rm eff}^2}=3.9\pm 0.1. \tag{85}$$

Estimating $\mu_{\rm eff}=4.8\mu_{\rm B}$ (Chattopadhyay *et al.*, 1989; Clinton *et al.*, 1995) yields a value of $T_N=0.47$ K, close to, though somewhat below, the observed value of $T_N=0.62$ K. To estimate the effect of the exchange interaction on the Néel temperature, we make the rather naive assumption that the exchange interaction is constant across the rare-earth series and hence

$$\mathcal{J}\propto\left(\frac{\mu_{\rm eff}}{S_{\rm eff}}\right)^2\propto\left(\frac{g_J-1}{g_J}\right)^2, \tag{86}$$

where g_J denotes the Landé *g* factor. Using the value for $\mathcal{J}$ obtained from the Dy data we obtain

$$\mathcal{J}(\mathrm{Er})=\frac{4}{9}\mathcal{J}(\mathrm{Dy})\approx 0.23. \tag{87}$$

Extending the above simulations to include the effect of the exchange interaction with $\mathcal{J}=0.23$ gives $T_N=0.57$ K, which lies within 10% of the measured value.

Given the significant anisotropy arising from the crystalline electric field in $DyBa_2Cu_3O_{7-\delta}$, comparing it with the results from the uniaxial model is quite appropriate. However, in the Er compounds, while it may be argued that such a model might be appropriate for the orthorhombic case, it is difficult to justify for the tetragonal case, in which the *a* and *b* axes are equivalent. Simulations for a pure dipolar spin system, in which the spins are confined to lie in the plane of the lattice, indicate that the spins do in fact order antiferromagnetically at finite temperature with a Néel temperature $2a^3k_BT_n/\mu_{\rm eff}^2=2.78\pm 0.10$ K (De'Bell *et al.*, 1997). As discussed in Sec. IV.B, this ordering arises from the anisotropic nature of the dipolar interaction, although the effect is complicated by the degeneracy of the ground state. From a theoretical perspective this suggests that both models can provide an adequate qualitative description of $ErBa_2Cu_3O_{7-\delta}$ and represent limiting cases of a more realistic description that includes finite anisotropy between the *x* and *y* axes. However, it is immediately apparent that such a description is at odds with the neutron-scattering results of Clinton *et al.* (1995), which do not show any long-range magnetic order down to the lowest temperatures in the tetragonal phase. This implies that the simple model does not provide an adequate description of these systems and that removing the oxygen does more than simply change the symmetry of the CEF anisotropy. Similarly, such a simple model is unable to account for the magnetic properties of $NdBa_2Cu_3O_{7-\delta}$, in particular, the fact that long-range molecular ordering is not observed for certain values of δ, suggesting that oxygen plays a more subtle role than one might naively suppose.

Despite the failure of this simple model in the case of erbium and neodymium, it can nevertheless be applied with some success to $GdBa_2Cu_3O_{7-\delta}$. As the ground state of Gd^{3+} is an *s* state, the crystalline electric fields are not expected to play a significant role. This is supported by heat-capacity measurements which show that the ground state of Gd^{3+} retains the full eightfold degeneracy of the free ion. Applying the scaling argument given by Eq. (86) yields the following value for *g*:

$$\mathcal{J}(\mathrm{Gd})=4\mathcal{J}(\mathrm{Dy})\approx 2.04. \tag{88}$$

Such a large value of the exchange-constant result implies that the ground state will be determined so as to minimize the exchange energy and will be similar to that observed experimentally (see Sec. II.B) in which the spins are aligned perpendicular to the *xy* plane and are ordered antiferromagnetically along both the *x* and *y* axes.

From the interpolation formula of Eq. (84), we obtain a value

$$\frac{2a^3 k_B T_n}{\mu_{\rm eff}^2} = 7.22. \tag{89}$$

Using a value of $\mu_{\rm eff} = 7.49\mu_B$ (Brown *et al.*, 1987; Paul *et al.*, 1988), this gives $T_N = 2.34$ K, which is very close to the observed value of 2.24 K.

We conclude, therefore, that while many of the properties of the $REBa_2Cu_3O_{7-\delta}$ may be successfully accounted for in terms of a simple model which consists of the dipolar interaction, CEF fields, and a simple nearest-neighbor exchange, the model nevertheless fails in certain critical ways. Most notably, it cannot account for the absence of long-range magnetic ordering in either $ErBa_2Cu_3O_6$ or $NdBa_2Cu_3O_{7-\delta}$, with $0.22 < \delta < 0.55$. The mixed success of this model suggests that the rare-earth sublattice cannot simply be considered in isolation as one might naively suppose. It would be useful, therefore, to extend previous analyses to include the coupling between the rare-earth sublattice and the CuO_2 planes. In particular, an examination of the role of hole doping in the CuO_2 planes and the effect of the superexchange, as suggested by Allenspach *et al.* (1995), would be of considerable interest.

B. Uniaxial ultrathin films

1. Stripe domains

As noted in Sec. II.A, for sufficiently thin films the magnetic moments in many systems are found to orient perpendicular to the plane of the film, indicating that the surface anisotropy is sufficient to overcome the anisotropy of the dipolar interaction, which favors in-plane ordering. Experimental studies such as those by Allenspach *et al.* (1990) and Allenspach and Bischof (1992) show that a characteristic of such out-of-plane ordering is the formation of domain patterns, in which the domains consist of ferromagnetically ordered groups of spins. Ground-state energy calculations (Garel and Doniach, 1982; Kaplan and Gehring, 1993; MacIsaac *et al.*, 1995), renormalization-group-based arguments (Kashuba and Pokrovsky, 1993b) and Monte Carlo simulations (Hurley and Singer, 1992a; MacIsaac, 1992; Booth *et al.*, 1995) all predict the existence of a striped phase at low temperatures for systems with dipolar interactions and exchange interactions that favor ferromagnetic ordering. Qualitatively, we can understand the stability of the stripe domains as a compromise between the increase in exchange energy due to the formation of domain walls and the decrease in the dipolar energy due to the interaction between magnetization currents generated at the domain walls. The equilibrium width of the domains is obtained by minimizing the total energy (exchange+dipolar) with respect to the stripe width. From the expression given in Table II for the dipolar energy of stripes of width l and the corresponding expression for the exchange energy $(-2(1-1/l))$, we obtain an equilibrium width given by

$$l^* = l_0 e^{J/4g}, \tag{90}$$

where l_0 is a constant of order one (Whitehead and De'Bell, 1994).

The stability of the striped phase has been considered by a number of authors. Earlier work cited by Abanov *et al.* (1995) appeared to indicate that striped crystals might be unstable with respect to small fluctuations; however, mean-field calculations show that the domain walls in the striped phase are stable (Abanov *et al.*, 1995; Castro, 1996). In addition to the mean-field properties, Chui has considered the effect of the pinning potential, due to the underlying lattice, on the finite-temperature properties of an array of domain walls (Chui, 1995b) and suggests that the renormalization of the potential can give rise to a roughening transition at some finite temperature.

For systems with exchange interactions sufficient to produce bulk Curie temperatures of several hundred Kelvin, the ground-state stripe width is predicted to be much larger than any practical laboratory sample size (Kashuba and Pokrovsky 1993a; Whitehead and De'Bell, 1994). This is consistent with experimental studies that observe a net ferromagnetic moment in the out-of-plane orientation at low temperatures (see Sec. II.A). Renormalization-group arguments (Kashuba and Pokrovsky, 1993b) indicate that as the temperature is increased the stripe width will decrease exponentially. Consequently there will exist a temperature at which the domain size becomes comparable with the size of the system and the net magnetization of the sample goes to zero due to the formation of stripe domains with alternating orientations.

2. Monte Carlo simulations

Although inherently limited to systems much smaller than experimental systems, Monte Carlo simulations can provide useful information on how domain structures are affected by parameters such as temperature.

Monte Carlo simulations of uniaxial ultrathin films on a square lattice exhibit a number of stages in the evolution of the system as the temperature is increased (Booth *et al.*, 1995). Typical spin configurations for this system at various temperatures are shown in Fig. 4. At low temperatures, the domain walls are essentially rigid until the thermal energy becomes of the order of the energy of an elementary excitation of the domain wall. As the temperature of the system is increased above this threshold temperature, the internal energy of the system rapidly increases and the fluidity of the walls also increases rapidly. However, the symmetry between the vertical (y) and horizontal (x) directions remains broken.

The breaking of this symmetry can be quantified by use of an order parameter O_{hv}, as introduced by Booth *et al.* (1995), and defined by

$$O_{hv} = \frac{n_h - n_v}{n}, \tag{91}$$

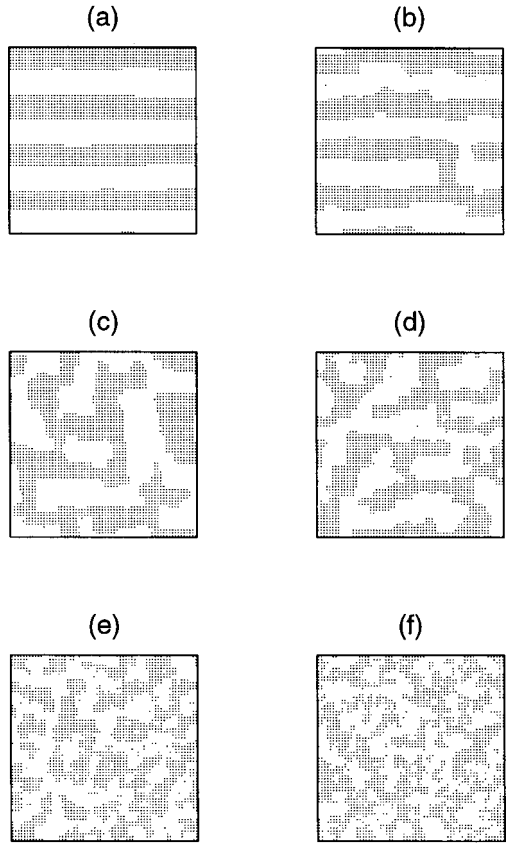

FIG. 4. Typical spin configurations for a uniaxial model on a square lattice with $J/g=8.9$. The configurations were generated in Monte Carlo simulations at temperatures $kT/g=(a)$ 3.0; (b) 4.8; (c) 5.2; (d) 6.4; (e) 10.0; and (f) 13.0. (c) shows the tetragonal phase which occurs just above the phase transition.

where n_h and n_v are the number of bonds between spins with opposite orientation which are parallel to the horizontal or vertical direction, respectively. Here, n is the total number of bonds between spins of opposite orientation. This order parameter is saturated at a value of 1 (or -1) in the striped ground state, but decays with temperature and decreases to zero continuously at a critical temperature T_c.

The vanishing of this order parameter signifies a restoration of the symmetry between the vertical and horizontal directions. Inspection of the spin configurations just above the critical temperature T_c reveals that the typical configurations consist of a patchwork of domains of spins of a given orientation (Fig. 4; Booth *et al.*, 1995). The interiors of the domains (patches) are highly stable and, typically, contain no spins of the opposite orientation at temperatures just above the critical temperature.

At still higher temperatures, this tetragonal phase decays into a fully disordered (''paramagnetic'') phase. However, no sharp phase transition between the tetragonal and paramagnetic phases is observed in Monte Carlo simulations for a square-lattice system. This contrasts with the prediction made by Abanov *et al.* (1995), based on a continuum model, of a clearly defined phase line between the two phases.

3. Temperature dependence of the domain structure

Combining the results summarized in the previous two subsections, we would expect the domain structures in experimental studies of magnetic films with strong uniaxial anisotropy to evolve through a number of stages. The first is a single-domain phase in which the system has a net magnetic moment. At a characteristic temperature, the film loses its magnetic moment due to the onset of multiple domains in the striped phase. In the striped phase the domains are oriented along a common crystallographic axis. As the temperature is further increased, the number of domains increases exponentially. In addition, as the thermal energy approaches a value comparable to the excitation energy of a spin at a domain wall, the ''fluidity'' of the walls increases dramatically. Finally, the striped phase is replaced by a phase in which the magnetic domains are no longer oriented along a common axis but instead manifest the symmetry of the underlying lattice. In the case of the square lattice, we refer to this as the tetragonal phase. As the temperature is further increased, the tetragonal phase decays into a true paramagnetic phase. The precise sequence of steps by which the system moves from the ordered striped phase to the tetragonal phase may depend critically on the underlying lattice. For example, a nematic phase is not observed in Monte Carlo simulations on a square lattice (Booth *et al.*, 1995) but is apparent in Monte Carlo simulations on a triangular lattice (Hurley and Singer, 1992a)

Experimental studies of systems that remain uniaxial (or are well below the reorientation transition temperature) are generally consistent with this picture. In particular, the direct images obtained by Allenspach *et al.* (1990) and Allenspach and Bischof (1992) show both striped phases and a phase with a strong qualitative similarity to the tetragonal phase found in simulations by Booth *et al.* (1995). Experimental studies that use magnetic measurements, rather than direct imaging, are somewhat more difficult to interpret but, again, are generally consistent with the picture described above (Pappas *et al.*, 1990; Berger and Hopster, 1996a, 1996b; Arnold and Venus, 1998).

Arnold and Venus (1998) have studied the real and imaginary parts of the ac susceptibility of iron films of less than 2.2ML on a Ni/W(110) substrate. (At less than 2.2ML the net moment in this system remains uniaxial out of plane until the disordered phase is reached.) In a range of temperatures below 250 K the nonzero imaginary part indicates the existence of remanence associated with domains with stiff walls. At a conventional ferromagnetic-to-paramagnetic transition, the disappearance of the imaginary susceptibility is accompanied by a peak in the real part. However, in the measurements of Arnold and Venus (1998) the peak in the real part of the susceptibility occurs approximately 20 K below the loss of remanence. Moreover, above the temperature at which the loss of remanence occurs, the real part of the susceptibility decays exponentially (apart from a small shift) with temperature. This is consistent

with the theory of Kashuba and Pokrovsky (1993a, 1993b), which relates the domain density, and hence the inverse susceptibility, to the exponential of temperature

$$\chi \propto n(T)^{-1} \propto e^{-\alpha T}. \tag{92}$$

Arnold and Venus (1998) find that the value of $\alpha = 0.037(1/\mathrm{K})$ obtained experimentally for iron is of the same order of magnitude as that which they calculate based on the results of Kashuba and Pokrovsky (1993a, 1993b; $\alpha = 0.07(1/\mathrm{K})$).

An exponential increase in the number of domains, and corresponding decrease in susceptibility, with temperature was obtained by Kashuba and Pokrovsky (1993a, 1993b) for a continuum model. In this model the softening of the domain walls is due to the weakening of the effective anisotropy as the reorientation transition is approached. As noted by Whitehead and De'Bell (1994), real systems are likely to be intermediate between the limiting cases of a continuum system in which the ultraviolet cutoff results from the finite width of the domain wall (as in the case studied by Kashuba and Pokrovsky, 1993a, 1993b) and that of a truly uniaxial system on a lattice in which the underlying lattice provides the cutoff. The close correspondence between the functional forms for the dipolar energy found in these two limiting cases (Yafet and Gyorgy, 1988; Kashuba and Pokrovsky, 1993a, 1993b; MacIsaac *et al.*, 1995; MacIsaac, 1997b) implies that the general case may be described in terms of crossover functions involving the lattice spacing and the domain wall width.

In particular, the exponential decay of the susceptibility at high temperatures but below the temperature at which the stripes disorder may also be obtained if the results of MacIsaac *et al.* (1995) for a uniaxial system on a square lattice are generalized to finite temperature using arguments analogous to those used by Kashuba and Pokrovsky (1993b). Treating the walls as flat at low temperatures, we can obtain the energy/spin of a spin configuration with majority stripes of width $l+\delta$ and minority stripes of width $l-\delta$ in the limit of small external fields. We find

$$E = E_F - \frac{(Ag - 2J + Bg\ln(l))}{l} - \frac{2\delta h}{l}, \tag{93}$$

where E_F is the energy of the system if ordered ferromagnetically, J is the strength of the exchange interaction, A and B are constants (see Table II), and h is the external field strength. (We have ignored higher-order terms in $1/l$.) Strictly speaking, the first two terms on the right-hand side of the equation above were derived only for the zero-field (equal-width-stripes) case by MacIsaac *et al.* (1995); however, as we consider here only the case of $h \to 0$ ($\delta \to 0$), we shall need here only the derivatives of E evaluated at the value of l that minimizes the energy in the zero-field case. The straightforward generalization of the results of MacIsaac *et al.* (1995) given above is therefore sufficient.

Denoting the stripe width that minimizes the zero-field energy by l^*, where (MacIsaac *et al.*, 1995; Whitehead and De'Bell, 1994)

$$l^* = l_0 \exp(2J/Bg) \tag{94}$$

and

$$l_0 = \exp(1 - A/B), \tag{95}$$

and expanding the change in energy due to a finite field to second order in δ, we obtain

$$\Delta E(h) = \frac{\delta^2 Bg}{2l^{*3}} - \frac{h\delta}{l^*}. \tag{96}$$

Minimizing the change in energy with respect to δ, we obtain

$$\delta/l^* = hl^*/Bg. \tag{97}$$

As δ/l^* is the magnetization/spin in units of the saturation magnetization, we find that the initial susceptibility is

$$\chi = \frac{\partial M}{\partial h} \propto l^* \propto \exp(2J/Bg). \tag{98}$$

The value of J/Bg is large for most transition metals studied in metal-on-metal systems and the value of l^* found is much larger than any realistic laboratory specimen. The system at low temperatures is therefore a single domain and the contribution to the susceptibility from domain walls is zero.

To generalize the above results to finite temperature, we note that fluctuations of the domain walls may be scaled out by renormalization-group arguments, which we shall assume result in a renormalized value for the ratio of the exchange and dipolar interaction strengths. For simplicity, we envisage a real-space renormalization-group rescaling in which lengths are rescaled by a factor equal to the linear dimension of a typical fluctuation of the domain wall. In the renormalized system the walls will then be flat. For large stripes, we may assume that the wall fluctuations, at temperatures well below the critical temperature, are essentially those of the corresponding exchange-only Ising model and occur over distances characterized by the correlation length of this Ising model. Further, for definiteness, we assume that for low temperatures the exponent of the correlation length can be approximated by its mean-field value (an assumption consistent with the simplifications made in the analysis above). Simple power-counting arguments for the invariance of the Hamiltonian under the rescaling then lead to the conclusion that the effective ratio of J/g is

$$\frac{J}{g}(T) = bJ(T_c - T)^{3/2}/g, \tag{99}$$

where b is a proportionality constant. Expanding this expression to leading order in T for $T \ll T_c$, we obtain the temperature dependence of the renormalized ratio to be used in the equation for χ:

$$\frac{J}{Bg}(T) \propto (1 - T/T_c)^{3/2} \approx 1 - 3T/2T_c. \tag{100}$$

Consequently we obtain

$$\chi = \chi_0 e^{-\alpha T}. \tag{101}$$

Despite the simplifying assumptions used to obtain this result here, the form of the result is quite general and independent of the specific assumptions introduced in the preceding analysis.

Here we have used the simplest possible arguments in order to make the source of the exponential dependence of χ transparent. Use of the full renormalization-group machinery would only change the precise value of parameters such as α in the above calculation; nonetheless the application of the full renormalization group to a generalized model which allows both Bloch domain walls and a uniaxial anisotropy would be of some interest. In particular, this might be used to calculate the forms of the crossover functions discussed by Whitehead and De'Bell (1994). To the best of our knowledge, such a calculation has not been published.

Although the functional forms for the zero-external-field equilibrium susceptibility are the same in the lattice and continuum models, the existence of a lattice can affect the dynamics of the domain walls and give rise to observable effects in low-temperature ac susceptibility measurements such as those performed by Arnold and Venus (1998). Such effects would be absent in a continuum model. In order to achieve the equilibrium value of δ, in response to an applied external field, the domain walls must move over the underlying lattice in finite steps through a series of excitations. In order to make these finite steps, the corresponding energy barrier must be overcome. If the thermal energy is large compared with the height of the typical barrier, the domain walls move freely and the simple exponential form obtained above is observed for all frequencies of the applied field. However, at lower temperatures the finite response time τ of the walls will result in an observable remanence (imaginary part of χ) for frequencies $\omega \leq 1/\tau$ and a decrease in the in-phase response (real part of χ). Arnold and Venus (1998) found that the form

$$\chi_{\rm obs} = \frac{(1+i\omega\tau)\chi_{\rm equ}}{1+(\omega\tau)^2}, \tag{102}$$

where $\chi_{\rm equ}$ denotes the static equilibrium susceptibility, reproduces the qualitative form of their data. Consequently, the position of the peak in the real part of the ac susceptibility on the temperature scale will depend on the frequency of the applied field.

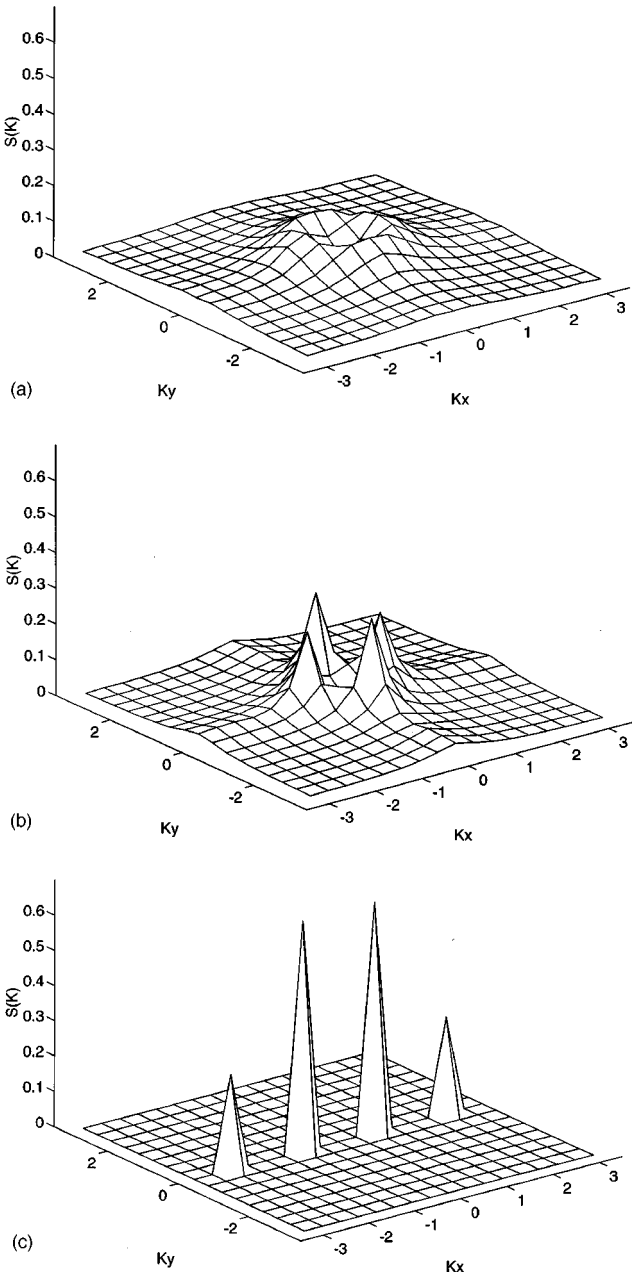

FIG. 5. Monte Carlo results for the variation of the structure factor with temperature for a uniaxial system on a square lattice (MacIsaac *et al.*, 1995), where $J/g = 5.5$. Structure factors are shown (a) well above the (smectic-to-tetragonal) transition temperature; (b) just above the transition temperature; and (c) below the transition temperature.

C. Temperature dependence of the structure factor

To analyze the changes in symmetry as the magnetic ordering changes, it is useful to calculate the structure factor $S(\vec{K})$:

$$S(\vec{K}) = \left\langle \left| \sum_{\vec{r}} \sigma(\vec{r}) \exp(i\vec{K}\cdot\vec{r}) \right|^2 \right\rangle. \tag{103}$$

The variation in the structure factor $S(\vec{r})$ with temperature may be observed during Monte Carlo simulations. In Fig. 5 we show this variation for a uniaxial system on a square lattice (MacIsaac *et al.*, 1995).

At low temperatures, the structure factor exhibits two primary peaks at $\pm\vec{q}$ on one of the principal axes of the Brillouin zone. (Subsidiary peaks are also observed due to the finite size of the basic replica cell in the simulation.) This is simply a reflection of the twofold symmetry of the striped phases. As the temperature passes through T_c into the tetragonal phase, the structure-factor pattern changes from two peaks on one of the axes to four peaks symmetrically placed on the two principal axes of the

Brillouin zone (Fig. 5). At temperatures just above T_c, the four structure-factor peaks remain sharp, indicating that the tetragonal domains have the symmetry of the underlying lattice and are quasiordered in the sense that this symmetry is maintained throughout the system and that the typical variation in the (linear) size of the domains is small compared with the average size of the domains.

As the temperature is further increased, the peaks become smeared into a circle giving the appearance of a four-peaked crown (Fig. 5). This feature in turn broadens, and at high temperatures it becomes indistinguishable from the background. This represents the loss of the fourfold symmetry of the tetragonal phase and its gradual replacement by the rotational symmetry of the paramagnetic phase. The tetragonal and paramagnetic phases are not separated by a sharp phase boundary; however, the change from one phase to the other may be accompanied by identifiable features in the thermodynamic properties.

This gradual change from the tetragonal to the paramagnetic phase symmetry in the structure factor is consistent with the specific-heat data obtained from Monte Carlo simulations. These measurements exhibit a broad peak well above the temperature at which the smectic-to-tetragonal transition occurs but below the critical temperature of the corresponding exchange-only Ising model (Booth *et al.*, 1995). That thermodynamic features, such as the rounded peak in the specific heat, correspond to the onset of pattern formation and the consequent change in symmetry, indicated by the structure factor, can be understood by considering how domains grow as the system is cooled from a high temperature. At sufficiently high temperatures, the system is truly paramagnetic with no stable domain cores; rather, groups of aligned spins have a linear dimension corresponding to the length scale on which correlated fluctuations occur and are therefore inherently unstable. In terms of the structure factor, a circular ridge indicates the characteristic size of the aligned groups, but the half-width of the ridge is as large as the radius of the ridge. As the temperature is lowered, the fluctuations and regions of aligned spins grow. Initially this mimics the growth of fluctuations in an exchange-only model, but the effective critical temperature of the model is lowered due to the competition between the dipolar interaction and the exchange interaction. Thus at high temperatures the specific-heat curve follows that for the exchange-only Ising model but is shifted to a lower temperature. As the temperature is further lowered, the dipolar interaction stabilizes adjacent regions of aligned spins, the domain cores form, and the fluctuations are restricted to the boundaries of the domains. Further lowering the temperature results in a decrease in the correlation length of the fluctuations as the domain cores stabilize and restrict fluctuations. As the specific heat corresponds to the fluctuations in the energy, we expect it to be maximal when the correlation length is maximal, i.e., at the onset of the stable tetragonal phase domains with linear dimensions greater than the fluctuation length. In the structure factor, this is mirrored by the onset of sharp peaks with fourfold symmetry.

D. Topological defects and the classification of phases

Up until now, the phases have been characterized primarily in thermodynamic terms, i.e., in terms of macroscopic averages such as the order parameter O_{hv} and the structure factor. This approach may be applied to a wide variety of physical systems both to analyze particular patterns and to draw analogies between pattern formation in different systems (Seul and Andelman, 1995). However, a complementary approach, which characterizes the phases in terms of topological defects, also provides considerable insight into pattern formation in a wide variety of systems. This approach has been applied to patterns obtained in experimental studies of various systems, such as thick ($\approx 10\,\mu$m) garnet films, by Seul *et al.* (1991) and Seul and Wolfe (1992).

The phases, of interest in the case of the magnetic thin films, may be characterized in terms of orientational order and the presence of two types of topological defects—dislocations and disinclinations (Abanov *et al.*, 1995). As these phases are analogous to those found in liquid crystals, the corresponding terminology is often used. At low temperatures, the stripes determine an orientational order, and there is also a spatial order which decays algebraically with distance. This smectic phase may contain bound pairs of dislocations, where a dislocation consists of the termination of a stripe and a corresponding distortion of the stripes around it, as shown schematically in Fig. 6.

By analogy with liquid crystals we might expect a transition from the smectic phase to a nematic phase at higher temperatures. In this phase, the orientational order is maintained but the spatial order decays exponentially. The transition from the smectic phase to the nematic phase is characterized by the unbinding of the dislocations. In addition, we might expect a tetragonal (square-lattice) or hexatic (triangular-lattice) phase to occur at still higher temperatures. In this phase, orientational order is lost and the pattern of magnetic moments has the symmetry of the underlying lattice. The dislocations that occur in the smectic and nematic phases may be considered to consist of a bound pair of disinclinations. A disinclination is the point at which two boundaries separating regions in which the stripes are oriented in different directions meet and terminate as shown in Fig. 6. The transition to the tetragonal (hexatic) phase is characterized by the unbinding of these disinclinations.

Abanov *et al.* (1995) have considered a continuum model of a thin magnetic film and predicted the possible phases. They conclude that the sequence of phases observed may be either smectic-nematic-tetragonal or smectic-tetragonal, depending on the parameters of the model. In the Monte Carlo simulations for a square lattice described above, only the smectic and tetragonal phases were observed by Booth *et al.* (1995). The Monte Carlo results appear to differ from the predictions of

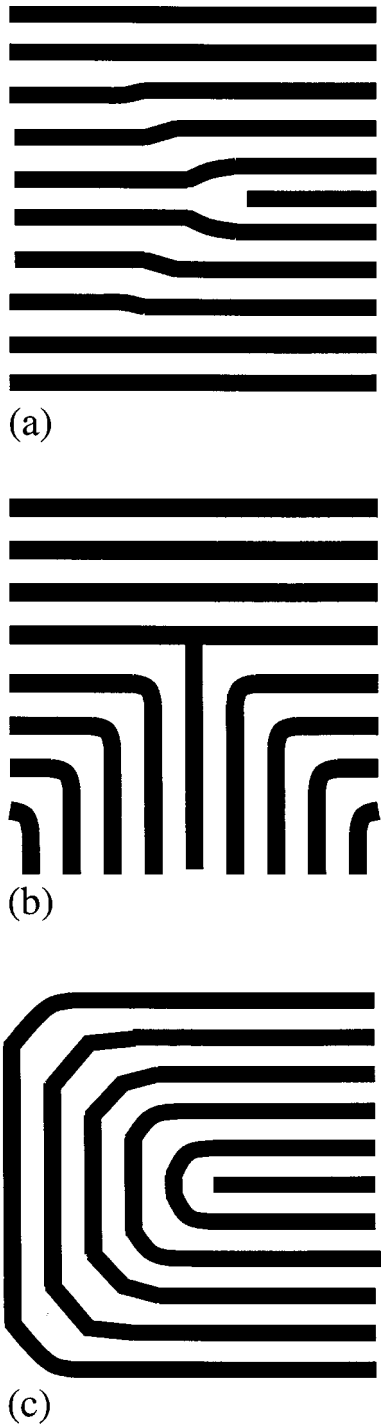

FIG. 6. Schematic representation of the (a) type of dislocation and (b),(c) types of disinclination that can occur in the striped phase.

Abanov *et al.* (1995) in that no discontinuity in the order parameter or hysteresis was observed at the smectic-to-tetragonal phase transition.

E. Finite external-field effects

In an applied external magnetic field, the results discussed in the previous subsections are modified by the competition between the antiferromagnetic order which

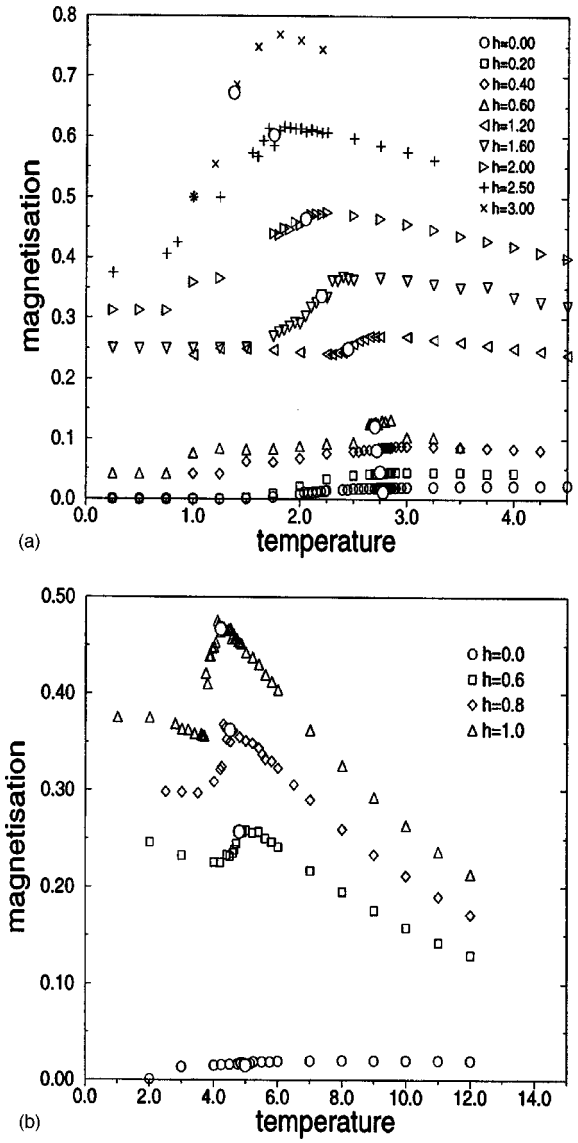

FIG. 7. Variation of the magnetization with temperature for a uniaxial system on a square lattice at several values of the external field h: (a) $J/g=6.0$ and a 32×32 periodicity; (b) $J/g=8.9$ and a 64×64 periodicity (Arlett *et al.*, 1996).

occurs in the zero-external-field case and the ferromagnetic state favored by the external field. At low temperatures and small magnetic fields, the system compensates for this increased competition by modifying the domain structure so that a majority phase and minority phase exist. In the smectic phase the stripes of the majority phase, favored by the applied field, are wider than the stripes of the minority phase; while in the tetragonal phase isolated domains of the minority phase are embedded in the majority-phase background (Arlett *et al.*, 1996).

A novel effect of the applied magnetic field is that when the temperature of the film is raised from zero temperature, its magnetization initially increases (Fig. 7). This can easily be understood as an analog of the Zeeman effect. Application of the field lowers the activation energy required for those fluctuations which increase the number of spins in the majority phase and

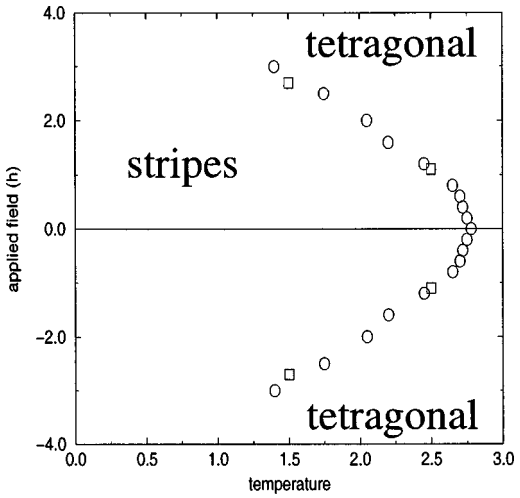

FIG. 8. Finite-external-field phase diagram obtained from Monte Carlo simulation of a uniaxial system on a square lattice (Arlett *et al.*, 1996).

increases the activation energy required for those fluctuations which increase the number of spins in the minority phase. This breaking of degeneracy between the two activation energies results in the observed increase in magnetization with temperature.

This continues until the thermal disordering of the majority phase overtakes the effect of the asymmetry and the magnetization begins to decrease. A related effect is the lowering of the critical temperature at which the smectic-to-tetragonal transition occurs, as the applied field reduces the width of the minority stripes and encourages the formation of ''bridges'' across the minority stripes by the majority phase. In simulations on small systems with stripe widths of 4 or 8 lattice spacings (in the zero-field case), the transition was found to occur at or below the temperature at which maximum magnetization occurred (Arlett *et al.*, 1996).

The phase diagram determined from Monte Carlo simulations on a square lattice is shown in Fig. 8. At low temperatures the transition from the smectic to the tetragonal phase shows hysteresis effects, indicating that the transition on this section of the phase boundary is first order. The transition appears to be second order at higher temperatures. However, due to the limited size of the system simulated, the possibility cannot be ruled out that the transition may be first order on the whole phase boundary, perhaps with a discontinuity in the order parameter which shrinks to zero in the limit of zero external field.

F. Constant order-parameter simulations

Hurley and Singer (1992a) have performed simulations in the alternate ensemble of fixed magnetization (or density, in the language of fluids). These simulations were performed using a modified sampling procedure in which spins near the domain walls were sampled much more frequently than those in the domain centers. The interpretation of such methods must be treated with some caution, as they may incorrectly treat disordering effects which are significant at higher temperatures. Nonetheless, the results are probably accurate at low temperatures, and this technique allowed Hurley and Singer to probe a low-temperature region in which the slow dynamics of conventional Metropolis-Boltzmann sampling would have made the simulation impractical. The results on the triangular lattice are particularly interesting as, in addition to a low-temperature bubble phase and smectic phase (Hurley and Singer, 1992b, 1992c), a nematic phase is apparent in finite-temperature simulations (Hurley and Singer, 1992a). This nematic phase is not observed in the simulations described above for the square lattice. In a continuum-theory approach, Abanov *et al.* (1995) found that the occurrence or nonoccurrence of this nematic phase between the smectic and tetragonal phases depended on a parameter of the model. This points again to the importance of the underlying lattice in determining the phase behavior of the system.

VI. REORIENTATION TRANSITION

As noted in Sec. II, the magnetic properties of several thin metal-on-metal films are remarkable in that they exhibit two distinct regions with a nonzero magnetization. Typically, a saturation magnetization in the direction perpendicular to the plane of the film occurs at low temperatures for sufficiently thin films. This decays as temperature is increased until a region of essentially zero magnetization is reached. If the temperature of the film is further increased, an onset of magnetization in a basal-plane direction is observed, and this saturates before decaying to a paramagnetic state at higher temperatures. Experimental results indicate that the region between the two regions with nonzero magnetization still has individual moments oriented (mainly) perpendicular to the plane of the film. However, the moments are arranged in domains such that the net magnetization of the system is essentially zero.

Increasing the thickness of the film at fixed temperature has a similar effect to increasing its temperature in that the orientation of the net magnetic moment is typically out of plane for very thin films but reorients to be (primarily) in plane once the film thickness exceeds a critical value. Although this sequence from out of plane to in plane with increasing film thickness is typical of most systems, the opposite sequence has also been observed. Schulz and Baberschke (1994) found that Ni on Cu(001) has an in-plane magnetic moment for films of less than 7 monolayers of Ni. Above a critical thickness of approximately 7 monolayers, the moment is perpendicular to the plane. This result is particularly interesting for potential applications to data storage, as thicker films are more reliably manufactured and less fragile but perpendicular-to-plane orientation is desirable for digital storage of data.

While the studies of uniaxial and planar systems described in the previous sections provide some understanding of the magnetic properties of these films in ap-

TABLE III. Typical calculated layer-resolved anisotropy energies $\Delta E = E^{\parallel} - E^{\perp}$ (see Sec. VI.A) for N-layer multilayers of Fe on Au (001) (Szunyogh *et al.*, 1995). Energies are expressed in meV/atom.

N	Fe(1)	Fe(2)	Fe(3)	Fe(4)	Fe(5)	Fe(6)	Au(1)	Au(2)
1	0.454						0.160	−0.002
2	0.034	0.522					0.027	0.015
3	0.168	−0.117	0.585				0.078	0.025
6	0.178	−0.031	−0.014	−0.033	−0.088	0.543	0.085	0.021

propriate ranges of temperature and film thickness, a complete description requires a detailed treatment of the surface anisotropy. The reorientation transition (also referred to as a switching transition in earlier work) is said to occur from the phase in which moments are aligned perpendicular to the plane to a phase in which the moments are predominately parallel to the plane. Experimentally the reorientation transition temperature is identified as the temperature at which the onset of the in-plane magnetization occurs.

Two features of these systems combine to produce the reorientation. The first is the breaking of the symmetry between in-plane and out-of-plane moment directions. This results from both the magnetocrystalline anisotropy and the inherent anisotropy of the dipolar interactions. It can be represented as a single-site effective-anisotropy term which stands for the difference in energy for spins aligned parallel to the plane from those aligned perpendicular to the plane,

$$K_{\mathrm{eff}} = K_{\mathrm{an}} + K_{\mathrm{dd}}, \tag{104}$$

where K_{eff} is the total effective, on-site anisotropy. K_{dd} is the difference in the thermally averaged energies due to the dipolar interactions between perpendicular-to-plane and in-plane orientations. K_{an} is the difference in energy due to magnetocrystalline effects.

The second feature determining the reorientation transition is the effect of cooperative phenomena. Such effects cannot always be incorporated into a single-site anisotropy but instead require a detailed analysis.

A. The effective anisotropy

Traditionally the effective anisotropy has been divided into two terms,

$$K_{\mathrm{eff}} = K_{\mathrm{V}} + K_{\mathrm{s}}/d. \tag{105}$$

The first term is independent of the film thickness d; however, both the volume term coefficient K_V and the surface term coefficient K_s may depend on temperature.

In early work, K_V was thought to depend only on the bulk values; however, surface effects such as strains induced by the substrate may effect K_V. Schulz and Baberschke (1994) found that for Ni/Cu(001) the surface value of K_V was two orders of magnitude larger than the corresponding bulk value. Also for fcc (111), (110), and (001) monolayer films, the change in energy with angle to the normal (θ) is found to vary as

$$\delta E = K_0 + K_2 \sin^2(\theta) \tag{106}$$

to lowest order (Bruno, 1989). [K_2 depends on the azimuthal angle in the case of (110) monolayers. For a more general expression see, for example, Bland *et al.* (1995).] For ferromagnetically ordered systems, the dipolar energy also varies as $\sin^2(\theta)$ (Szunyogh *et al.*, 1995).

Although calculations for isolated monolayers may give some sense of the magnitude of the magnetocrystalline surface anisotropy, in metal-on-metal films the presence of the substrate is likely to significantly modify the anisotropy in the over-layers. Szunyogh *et al.* (1995) have used the Korringa-Kohn-Rostoker method to calculate the magnetocrystalline anisotropy in multilayers of Fe on a Au(001) substrate for numbers of layers from 1 to 6. We summarize some of the results in Tables III and IV.

The results of Szunyogh *et al.* (1995) show several interesting features. The energy difference between in-plane and out-of-plane ordering is positive (i.e., favors out-of-plane ordering) only for the outermost Fe layer and for the layer immediately adjacent to the gold substrate. For intermediate layers, the single-atom energy difference would favor in-plane ordering. In all cases, the energy difference is significantly larger for the layer adjacent to the gold than for the other Fe layers. Simi-

TABLE IV. Typical calculated layer-resolved changes in orbital magnetic moments $\Delta m_{\mathrm{orb}} = m^{\parallel}_{\mathrm{orb}} - m^{\perp}_{\mathrm{orb}}$ (see Sec. VI.A) for N-layer multilayers of Fe on Au (001) (Szunyogh *et al.*, 1995). Changes are expressed in $10^{-3}\mu_B$.

N	Fe(1)	Fe(2)	Fe(3)	Fe(4)	Fe(5)	Fe(6)	Au(1)	Au(2)
1	−29.1						2.9	1.3
2	5.1	−37.3					6.3	1.2
3	8.3	−7.9	−30.2				2.9	0.9
6	3.6	0.5	−2.2	3.7	−0.3	−26.3	2.4	0.7

larly, the calculated difference in the out-of-plane and in-plane orbital magnetic moments is far larger for the layer adjacent to the substrate than for the other Fe layers. Szunyogh *et al.* (1995) find that there is no straightforward relationship between the anisotropy in the orbital magnetic moments and the corresponding anisotropy energies. They conclude that the relationship between the orbital magnetic moments and the magnetic anisotropy energies is much more complicated for multilayer systems than that found for a single monolayer by Bruno (1989).

Szunyogh *et al.* (1995) also find that the magnetocrystalline anisotropy $K_{\rm an}$ remains almost constant as the number of layers increases; however, the magnitude of the dipolar anisotropy increases rapidly with film thickness. Consequently $K_{\rm eff}$ changes sign at $d \approx 3.3$ML and for films thicker than this favors orientation of the moments in the plane. This can be compared with the critical thickness for reorientation of $d \approx 2.8$ML found experimentally (Liu and Bader, 1990).

Lessard *et al.* (1997) calculated the magnetocrystalline anisotropy energy for films of Fe on Cu(001) and for Ni on Cu(001). In each case the energies were calculated for films with up to 14 layers. In these calculations, the role of the substrate was modeled by adjusting the spacing in the film to match that expected for epitaxial growth on Cu(001). In the case of Fe, Lessard *et al.* (1997) found the magnetic anisotropy favored out-of-plane orientation for thin films with a switch to in-plane ordering being favored at 4ML. This is in good agreement with observations of a reorientation transition between 4 and 5 ML. This result implies that the reorientation transition is not driven by the restructuring of the film, which is also observed at approximately 5ML. However, the structural phase changes appear to be closely correlated with the changes in magnetic phase (Li *et al.*, 1994; Müller *et al.*, 1995; Zharnikov *et al.*, 1996) and the link between them is still not fully understood. For the Ni films, Lessard *et al.* (1997) find that the anisotropy favors in-plane ordering for thin films. This is consistent with the observations of Schulz and Baberschke (1994) for this system. However, Lessard *et al.* (1997) do not find a reorientation to out-of-plane ordering at 7ML as observed by Schulz and Baberschke (1994).

The extension of the *ab initio* and band-theory calculations to finite temperature is difficult to achieve in a reliable manner. Experimentally, the temperature dependence of the magnetocrystalline anisotropy may be determined from UHV-ferromagnetic-resonance (FMR) measurements (Baberschke, 1996). The resulting data may be decomposed into volume and surface terms, as discussed above. Two systems for which such measurements are available and which typify the possible sequences of phases at the reorientation transition are Gd(0001) on W(110) and Ni on Cu(001) (Baberschke, 1996; Farle, Platow, *et al.*, 1997).

The Gd(0001)-on-W(110) system is typical of almost all ultrathin films which exhibit the reorientation transition, having an out-of-plane moment orientation at low temperatures and an in-plane moment above the reorientation transition temperature. Experimental observations find for the Gd film that the contribution to K_s from the magnetocrystalline anisotropy favors out-of-plane orientation of the moments. K_s appears to be a linear function of temperature and can be extrapolated to $K_s(T=0\ {\rm K}) = 2.8$ meV/atom. K_V favors in-plane orientations at low temperatures but is smaller than K_s (in the temperature region where measurements are available). K_V is observed to change sign at approximately 0.65 of the Curie temperature.

The Ni-on-Cu (001) system is atypical, exhibiting an in-plane orientation at low temperatures and an out-of-plane orientation above the reorientation transition temperature. Baberschke (1996) noted that the reorientation transition occurs only in a narrow range of film thicknesses of $d \approx 7$ML. In this Ni film, the magnetocrystalline contribution to K_s favors orientation in the plane. Since this is also the orientation favored by the dipole energy, it might be expected that no reorientation transition would take place. However, in this system K_V is anomalously large (compared with the bulk value; Schulz and Baberschke, 1994) and favors out-of-plane ordering at all temperatures below the Curie temperature (Farle, Platow, *et al.*, 1997). The anomalous (continuous) appearance of an out-of-plane orientation of the moments above the critical thickness and above the reorientation transition temperature can therefore be understood in terms of the unusual role played by the volume anisotropy term. FMR measurements of K_V and K_s for Ni on W(110) show that they behave in a qualitatively similar way to their counterparts in Ni/Cu(001) but that K_V is significantly smaller than that found in Ni/Cu(001). Values of K_s are very close for the two systems. [For a detailed discussion of the angular dependence of the magnetic moment on film thickness in Ni/Cu(001), see also Farle, Mirwald-Schulz, *et al.* (1997)].

Farle, Platow, *et al.* (1997) have emphasized the importance of magnetoelastic effects in producing the differences in behavior of these systems. They noted that Ni on Cu(001) grows pseudomorphically up to 10 ML with a lattice expansion of 2.5% compared to bulk Ni. Consequently, even for the thicker films in this range, there is no strain relaxation by the incorporation of a dislocation network. This contrasts with the behavior of Gd and Ni on W(110), where the lattice mismatch is much larger. Farle, Platow, *et al.* (1997) observe that the magnitude and temperature dependence of K_V for Ni/Cu(001) can be explained by the 2.5% strain in a magnetoelastic model and by the temperature dependence of the magnetostrictive and elastic constants. Unfortunately, it is not clear how to extrapolate the measurements of Farle, Platow, *et al.* (1997) to zero temperature for Ni/Cu(001). Consequently it is not possible to make a direct comparison of the values of K_V and K_s obtained experimentally with those calculated by Lessard *et al.* (1997). Lessard *et al.* (1997) correctly predicted the in-plane orientation at low temperatures in thin films, based on a model in which the substrate was represented through a change in the lattice spacing in the film. This

model appears to be consistent with the magnetoelastic approach taken by Farle, Platow, *et al.* (1997). It is thus surprising that Lessard *et al.* (1997) did not see a change in the preferred out-of-plane anisotropy for thicker films. Lessard *et al.* (1997) speculated that this was due to subtle many-body effects, which are ignored by the commonly used "force theorem" (Weinert, Watson, and Davenport, 1985; Bylander and Kleinman, 1995).

B. Cooperative effects

As before, it is convenient to divide the theoretical studies into essentially two groups: those in which the exchange interaction is large compared with the dipolar interaction (Chui, 1994; Hucht, Moschel, and Usadel, 1995) and those studies in which the exchange interaction is negligible or comparable with the dipolar interaction (MacIsaac *et al.*, 1996; MacIsaac, 1997a; MacIsaac, De'Bell, and Whitehead, 1998). In practice these two ranges may be differentiated by noting that for systems with magnetic moments oriented perpendicular to the plane and reasonably large values of the exchange interaction the zero temperature stripe domains will be much larger than the size of the system (Kashuba and Pokrovsky, 1993b, Whitehead and De'Bell, 1994). This is consistent with experimental observations which see a single, out-of-plane domain at very low temperatures (Allenspach and Bischof, 1992). However, for values of the exchange interaction strength that are smaller than or comparable with the dipolar interaction strength, the stripe width will be smaller than the system size even at zero temperature, and the domain structure will be observable at the lowest temperatures probed.

The essential elements of the reorientation transition were discussed by Pescia and Pokrovsky (1990), who argued that although the on-site anisotropy favoring the perpendicular-to-plane orientation may be dominant at low temperatures, the magnitude of the dipolar anisotropy, favoring in-plane orientation, decreases more slowly than the on-site anisotropy with temperature. Jensen and Bennemann (1990, 1992) have argued that the increased entropy in the planar orientation also plays a key role in the reorientation transition and that, even if the magnitude of this term is small in the free energy, it makes possible a second-order transition rather than the first-order transition predicted by Pescia and Pokrovsky (1990).

We may then define a temperature T_R (for given K) such that, if T is varied, T_R is the temperature at which the difference in free energy between the in-plane and perpendicular phases changes sign. If T_R is less than the Curie temperature, then a reorientation transition is observed.[3] Subsequently, Chui (1994), and Hucht and Usadel (1996) used Monte Carlo calculations to locate the reorientation transition for various values of the on-site anisotropy in this limit of large exchange interactions.

In the opposite extreme of zero exchange interaction, MacIsaac *et al.* (1996) used Monte Carlo calculations to show that a reorientation transition also occurs. In the absence of an exchange interaction, the system starts from an antiferromagnetic ground state if the effective anisotropy favors an in-plane configuration. If the effective anisotropy favors out-of-plane orientations, then the ground state is a simple antiferromagnetic arrangement. The ratio of the on-site anisotropy parameter to the dipolar interaction parameter at which the system switches from its in-plane state to the out-of-plane state is calculated (exactly) to be $K/g=2.44$. As the temperature is increased, the value of the ratio K/g at which the reorientation occurs decreases. This is the opposite to what happens in the large-exchange-interaction limit. MacIsaac (1997a) and MacIsaac *et al.* (1998) have considered the effect of adding an exchange interaction comparable with the dipole parameter strength $J/g=6$. This changes the ground state to a striped phase for large K_{eff} and to an in-plane ferromagnet for small K_{eff}. For this value of J/g, despite the change in the ground states, the value of $K(T)$ at which reorientation occurs is still a decreasing function of temperature, as in the $J/g=0$ case. However, it should be noted that the nonuniform sampling technique used by MacIsaac *et al.* in these studies resulted in an additional temperature dependent effective anisotropy (MacIsaac *et al.*, 2000).

C. Phase diagrams

Phase diagrams based on studies of systems with large (Hucht *et al.*, 1995), small (MacIsaac *et al.*, 1998), and zero exchange interactions (MacIsaac *et al.*, 1996) are shown in Figs. 9, 10, and 11, respectively. All three show a reorientation transition that is first order in nature for a single-monolayer system. [The study by Chui is the only simulation study that predicts a continuous transition (Chui, 1994)]. Usadel and co-workers have investigated how the first-order or second-order nature of the transition is determined by the distribution of anisotropies through the thickness of the film (Moschel and Usadel, 1995; Hucht and Usadel, 1996).

In addition to the zero-external-magnetic-field studies reviewed above, Berger and Erickson (1997) have recently introduced a five-parameter mean-field model which incorporates the effects of both the stripe domains and an external magnetic field in a system close to the reorientation transition. The results obtained for a 4ML system give very good qualitative agreement with those obtained experimentally for a 3.8ML Fe on Ag(100) film.

The qualitative agreement between the phase diagrams obtained by simulations and the sequences of phases observed experimentally is quite satisfactory, in the sense that horizontal lines corresponding to temperature scans can be drawn which reproduce the se-

[3]Note that, though the qualitative arguments given by Pescia and Pokrovsky (1990) establish the physical basis for the reorientation transition, the quantitative results in their paper are not correct. See the comment by Levanyuk and Garcia (1993) and the reply by Pescia and Pokrovsky (1993).

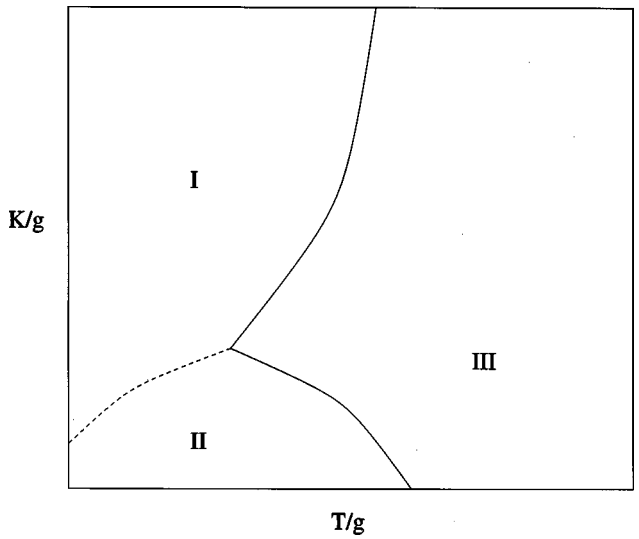

FIG. 9. Schematic phase diagram for a film with $J/g \gg 1$ based on Hucht *et al.* (1995): solid curves, continuous transitions; dashed curves, first-order transitions. The labeled phases are I, out-of-plane ferromagnetic; II, in-plane ferromagnetic; and III, disordered.

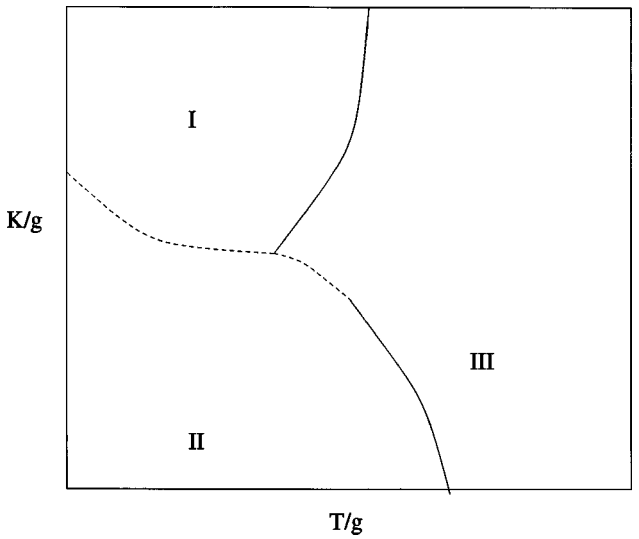

FIG. 11. Schematic phase diagram for a film with $J/g \sim 1$ after MacIsaac *et al.* (1998): solid curves, continuous transitions; dashed curves, first-order transitions. Phases are I, out-of-plane smectic; II, in-plane ferromagnetic; and III, tetragonal/disordered.

quences of phases obtained experimentally when temperature is varied at constant thickness (Pappas *et al.*, 1990; Allenspach and Bischof, 1992; Berger and Hopster, 1996a). Similarly, a vertical line drawn on the phase diagram represents varying magnetocrystalline anisotropy at constant temperature; this can be achieved in experimental studies by varying the thickness of the film at constant temperature. A vertical line can be drawn on the phase diagram that reproduces the sequence of phases observed experimentally (Allenspach *et al.*, 1990). Two caveats must be given. First, the use of horizontal and vertical lines on the phase diagrams to represent experimental temperature scans at fixed thickness and thickness scans at fixed temperature is a considerable oversimplification. The magnetocrystalline anisotropy depends in a nontrivial way on temperature, as demonstrated by ferromagnetic resonance measurements (Farle, Platow, *et al.*, 1997). Moreover, the effective strength of the local dipolar field (which determines the effective temperature scale in the simulations) depends on the thickness of the film. [Hucht and Usadel (1997) have recently calculated the temperature variation for Ni on Cu(001) within a mean-field approach]. Second, in studies that do not use direct imaging of the domains, it has generally been assumed that the domain phase with zero net magnetization is the striped domain phase only (Berger and Hopster, 1996a). In fact, studies that image domains directly do appear to show the presence of tetragonal domains (Allenspach *et al.*, 1990).

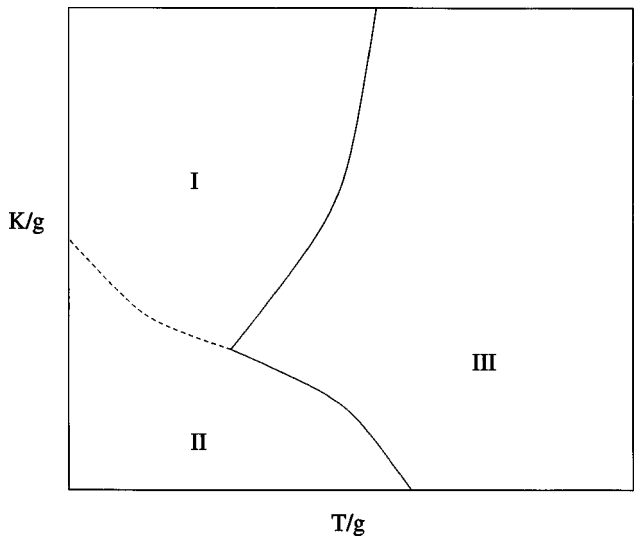

FIG. 10. Schematic phase diagram for a film with $J/g = 0$ after MacIsaac *et al.* (1996): solid curves, continuous transitions; dashed curves, first-order transitions. Phases are I, out-of-plane antiferromagnetic; II, in-plane antiferromagnetic; and III, disordered.

In the following section we shall comment on experiments that probe domain dynamics and that, possibly, distinguish between equilibrium domain phases. These are obviously of great interest, since static magnetic measurements do not appear to distinguish between domain phases such as the smectic and tetragonal phases.

Despite these caveats, the qualitative agreement between the experimental and theoretical studies reviewed above confirms that models which contain exchange, magnetocrystalline, and dipolar interactions are necessary but not necessarily sufficient to explain the mesoscopic ordered structures and phase behavior obtained in ultrathin magnetic films as well as the long ranged ordered structures in quasi-two-dimensional systems such as the layered rare-earth compounds.

VII. DISCUSSION

We have summarized some key experimental results for an important class of layered rare-earth compounds,

$REBa_2Cu_3O_{7-\delta}$, and ultrathin metal-on-metal magnetic films. The ordered states in the rare-earth compounds consist of relatively simple antiferromagnetic ground states with a unit cell on the atomic length scale. In the case of the metal-on-metal magnetic films, much of the experimental work has focused on ferromagnetic compounds. Such systems exhibit a rich variety of phases. In the case of uniaxial systems, in which the spins are aligned perpendicular to the plane, domain structures on mesoscopic length scales have been observed and, in a number of important cases, a switching or reorientation transition from a uniaxial phase to a planar phase has been observed, in which the orientation of the spins changes from perpendicular to parallel to the plane. Such a transition can be induced by changing the temperature, applied external fields, or film thickness.

The simplest model that might describe the magnetic properties of each of these two groups of systems consists of a short-range exchange interaction and a dipolar interaction as well as a single-site term representing the magnetocrystalline anisotropy. We have reviewed results obtained from a number of theoretical and numerical studies of such a model system and have shown that, despite the simplicity of such a model, it manifests a wide variety of behaviors and can provide a consistent picture of many aspects of these systems.

Pattern formation, as occurs in the case of the magnetic domain states in thin metal-on-metal films, resulting from competition between a local interaction and the long-ranged exchange interaction, is common to a wide range of systems. Other systems that exhibit pattern formation of this type include ferroliquids, micrometer-thick magnetic garnet films, and Langmuir films (Seul and Andelman, 1995). For other materials, including shape-memory alloys, pattern formation may also result from competition between long-ranged and local interactions; however, the long-ranged interaction may be even more persistent than the dipolar interaction (Löw *et al.*, 1994; Saxena *et al.*, 1997). Despite the common occurrence of pattern formation as a result of competition between long-ranged and short-ranged interactions, it is difficult to identify a typical system. Even within the metal-on-metal films, features such as the existence of an underlying lattice and the structure of that lattice may determine which domain phases are observed in these inherently frustrated systems. Consequently, although analogies between continuum and lattice systems and between, say, metal-on-metal-film magnetic phases and liquid-crystal phases are useful, they must be treated with some caution (for a more complete discussion, see Sec. V).

The underlying lattice may also play a critical role in determining the dynamics of metal-on-metal films. We might expect two types of dynamical processes to occur in these systems. In one, individual (but correlated) spin flips will be the primary mechanism for the dynamics; in the other, it is the motion and relaxation of domains. This latter type of dynamics is likely to be much slower than the former type and poses interesting questions about metastability of domain phases and aging processes in these systems.

Some experimental studies already indicate the importance of domain dynamics in these systems (Berger and Hopster, 1996b; Arnold, Dunlavy, *et al.*, 1998; Arnold and Venus, 1998). Indeed, by studying the variation of the dynamical relaxation time with temperature, Arnold *et al.* (1998) inferred the temperature of the smectic-to-tetragonal transition from a change in the activation energy. Inspection of Fig. 2 of Berger and Hopster (1996b) shows a similar change in activation energy (slope of the Arrhenius plot). Although the experiment is different from that of Arnold *et al.* (1998), the change in activation energy may also be associated with a smectic-to-tetragonal transition.

Sampaio, Alburquerque, and de Menezes (1996) have performed Monte Carlo simulations of uniaxial out-of-plane systems on a square lattice relaxing from the saturated ferromagnetic state. Although there are difficulties in relating the Monte Carlo time (as measured by Monte Carlo steps) to actual times, such studies provide some insight into the dynamical behavior. In particular, Sampaio *et al.* (1996) conclude that the relaxation process separates into two distinct regimes, depending on the ratio of the exchange to the dipolar interaction. If the dipolar interaction dominates, then a single spin flip becomes energetically favorable and the magnetization decays as $t^{-\gamma}$. In the other regime, the exchange interaction dominates and a single spin flip is no longer energetically favorable; then the relaxation process is dominated by domain formation and growth, and the magnetization decays exponentially. More recent studies by Rappoport *et al.* (1998) have examined in more detail the effect of a magnetic field aligned opposite to the initial magnetization, on the relaxation process. Based on their numerical studies, Rappoport *et al.* (1998) conclude that, for sufficiently small magnetic fields, the zero-field picture remains valid, while, in the case of high fields, the magnetization exhibits only an exponential decay. Moreover, their results also indicate that the fractal dimension of the domain walls increases with increasing field. Toloza, Tamarit, and Cannas (1998) have studied the same model but in the case where the system is quenched from a high-temperature configuration to a subcritical temperature. Of particular interest is the conclusion of Toloza *et al.* (1998) that, for systems with comparable exchange and dipolar interaction strengths, there exists a region of slow relaxation dynamics possibly similar to those in other frustrated systems. Similar studies were previously performed by Desai and coworkers using Langevin dynamics for a model with a continuous uniaxial "spin" variable, that included a long-range interaction that could be varied between the dipolar and Coulombic forms depending on a parameter in the model (Roland and Desai 1990; Sagui and Desai, 1994).

It should be noted that the numerical studies on the kinematics of the uniaxial dipolar Ising model discussed above were perfomed largely using open rather than pe-

riodic boundary conditions for the dipolar interaction. Sampaio *et al.* (1996) state that a comparison between the semiopen boundary conditions (open for the dipolar interaction and periodic for the exchange interaction) and the periodic boundary conditions for a 32×32 lattice shows little observable difference. However, it is nevertheless the case that the treatment of the boundaries may affect the nucleation process significantly and, in the case of large stripe widths (i.e., $J\gg g$), the relaxation process at long times.

Despite the tremendous progress that has occurred in the last decade in both theoretical and experimental understanding of two-dimensional and quasi-two-dimensional magnetic systems, there nevertheless remain several intriguing and important questions. For example, in the domain phases, the role of the transverse component of the spin in the process of domain nucleation and growth is poorly understood, yet it will certainly play an important role in determining the nonequilibrium properties of these systems. Moreover, there is much that can be learned from the analogy between phases that occur in magnetic systems and those that occur in other frustrated or metastable systems such as supercooled liquids (Kivelson *et al.*, 1995). The rapid development in the fabrication and characterization of ultrathin films over the last decade, combined with advances in our understanding of the factors that determine magnetic properties of surface atoms, opens the way for a number of exciting technological applications. While much effort to date has focused on the magnetic properties of individual surface atoms and their interactions, the collective behavior of surface atoms is an essential factor in determining the basic properties of these systems. An example of this is the role of domain nucleation, growth, and dynamics in determining the magnetic response to an applied field. Despite the many recent advances described in this review, cooperative behavior in magnetic ultrathin films is nevertheless poorly understood, and the challenge is to develop techniques and approaches that will allow us to better describe the collective processes involved. This poses questions of a very basic nature regarding the equilibrium and nonequilibrium behavior of two-dimensional magnetic systems and the often subtle interplay between different interactions. Any significant progress will require a synthesis of theoretical analysis, numerical simulation, and detailed and systemic experiments.

Note added. After submission of this manuscript, the authors received a preprint by Stoycheva and Singer (Stoycheva, A. D., and S. J. Singer, ''Stripe melting in a two-dimensional system with competing interactions,'' Ohio State University preprint). Using a non-Metropolis Monte Carlo algorithm and a multipole expansion to treat the long-range part of the dipolar interaction, these authors determine the critical temperature at which the twofold order of the striped phase is lost for a triangular lattice of spins with orientation perpendicular to the plane. The authors provide an analytic scaling theory. Comparison of the results with results for the square lattice (summarized in this review) appears to confirm that the lattice structure plays a significant role in determining the phases and related phase transitions available to the system.

In a private communication, Professor Singer also drew our attention to the maxima observed in the magnetization as a function of temperature at constant external magnetic field, in Fig. 3 of Arlett *et al.* (1996). If the sharp increases in magnetization just below the maximum are assumed to be discontinuities in the limit of large systems, this would tend to support the conjecture of Arlett *et al.* (1996) that the transition is first order for any finite field, even though hysteresis loops were not observable in the small-field Monte Carlo data.

ACKNOWLEDGMENTS

The authors would like to acknowledge useful discussions with Dr. P. H. Poole and Dr. T. Lookman of the Department of Applied Mathematics at the University of Western Ontario and to thank Dr. D. Venus (McMaster University) and Dr. C. S. Arnold (Virginia Commonwealth University) for providing us with copies of their experimental results prior to publication. Earlier correspondence from Dr. A. Berger (University of California) also helped to draw our attention to the importance of dynamical studies. We would also like to acknowledge the contributions of our former students: Jessica Arlett (Caltech), Ivan Booth (Waterloo University), Samuel Bromley (Memorial University), and Michael Robertson (Trent University). This work was supported in part by the Natural Sciences and Engineering Research Council of Canada.

REFERENCES

Abanov, A., V. Kalatsky, V. L. Pokrovsky, and W. M. Saslow, 1995, Phys. Rev. B **51**, 1023–1038.

Allenspach, R., and A. Bischof, 1992, Phys. Rev. Lett. **69**, 3385–3388.

Allenspach, P., B. W. Lee, D. A. Gajewski, V. B. Barbeta, M. B. Maple, G. Nieva, S.-I. Yoo, M. J. Kramer, R. W. McCallum, and L. Ben-Dor, 1995, Z. Phys. B **96**, 455–464.

Allenspach, P., B. W. Lee, D. A. Gajewski, and M. B. Maple, 1994, Physica C **235–240**, 1735–1754.

Allenspach, R., M. Stampanoni, and A. Bischof, 1990, Phys. Rev. Lett. **65**, 3344–3347.

Arlett, J., J. P. Whitehead, A. B. MacIsaac, and K. De'Bell, 1996, Phys. Rev. B **54**, 3394–3402.

Arnold, C. S., M. Dunlavy, D. Venus, and D. P. Pappas, 1998, ''Magnetic susceptibility analysis of the relaxation time for domain-wall motion in perpendicularly magnetized ultrathin films,'' Preprint (McMaster University).

Arnold, C. S., H. L. Johnston, and D. Venus, 1997, Phys. Rev. B **56**, 8169–8174.

Arnold, C. S., and D. Venus, 1998, IEEE Trans. Magn. **34**, 1039.

Baberschke, K., 1996, Appl. Phys. A: Solids Surf. **62**, 417–427.

Baberschke, K., M. Farle, and M. Zomach, 1987, Appl. Phys. A: Solids Surf. **44**, 13–18.

Baudelet, F., M.-T. Lin, W. Kuch, K. Meinel, B. Choi, C. Schneider, and J. Kirscher, 1995, Phys. Rev. B **51**, 12563–12578.
Berger, A., and R. P. Erickson, 1997, J. Magn. Magn. Mater. **165**, 70–73.
Berger, A., and H. Hopster, 1996a, J. Appl. Phys. **79**, 5619–5621.
Berger, A., and H. Hopster, 1996b, Phys. Rev. Lett. **76**, 519–522.
Binder, K., and D. W. Heermann, 1993, *Monte Carlo Simulation in Statistical Physics*, second edition (Springer, Berlin).
Bland, J. A. C., C. Daboo, G. A. Gehring, B. Kaplan, A. J. R. Ives, R. J. Hicken, and A. D. Johnson, 1995, J. Phys.: Condens. Matter **7**, 6467–6476.
Bloch, F., 1928, Z. Phys. **49**, 206–219.
Bonsall, L., and A. Maradudin, 1977, Phys. Rev. B **15**, 1959.
Booth, I. N., A. B. MacIsaac, K. De'Bell, and J. P. Whitehead, 1995, Phys. Rev. Lett. **75**, 950–953.
Brown, S. E., J. D. Thompson, J. O. Willis, R. M. Aikin, E. Zirngiebl, J. L. Smith, Z. Fisk, and R. B. Schwarz, 1987, Phys. Rev. B **36**, 2298–2300.
Bruno, P., 1989, Phys. Rev. B **39**, 865–868.
Bruno, P., 1991, Phys. Rev. B **43**, 6015–6021.
Bylander, D. M., and L. Kleinman, 1995, Phys. Rev. B **52**, 1437–1440.
Callen, H. B., 1963, Phys. Rev. **130**, 890–898.
Castro, J., 1996, Phys. Lett. A **214**, 307–312.
Chattopadhyay, T., P. J. Brown, B. C. Sales, L. A. Boatner, H. A. Mook, and H. Maletta, 1989, Phys. Rev. B **40**, 2624–2626.
Chui, S. T., 1994, Phys. Rev. B **50**, 12559–12567.
Chui, S. T., 1995a, Phys. Rev. Lett. **74**, 3896–3899.
Chui, S. T., 1995b, Phys. Rev. B **51**, 250–257.
Clinton, T. W., and J. W. Lynn, 1991a, J. Appl. Phys. **70**, 5751–5753.
Clinton, T. W., and J. W. Lynn, 1991b, Physica C **174**, 487–490.
Clinton, T. W., J. W. Lynn, J. Z. Liu, Y. X. Jia, T. J. Goodwin, R. N. Shelton, B. W. Lee, M. Buchgeister, M. B. Maple, and J. L. Peng, 1995, Phys. Rev. B **51**, 15429–15447.
Corciovei, A., 1963, Phys. Rev. **130**, 2223–2229.
Corruccini, L. R., and S. J. White, 1993, Phys. Rev. B **47**, 773–777.
Daalderop, G. H. O., P. J. Kelly, and F. J. A. den Broeder, 1992, Phys. Rev. Lett. **68**, 682–685.
Daalderop, G. H. O., P. J. Kelly, and M. F. Schuurmans, 1990, Phys. Rev. B **42**, 7270–7273.
Daalderop, G. H. O., P. J. Kelly, and M. F. Schuurmans, 1991, Phys. Rev. B **44**, 12054–12057.
De'Bell, K., and D. J. W. Geldart, 1989, Phys. Rev. B **39**, 743–744.
De'Bell, K., A. B. MacIsaac, I. N. Booth, and J. P. Whitehead, 1997, Phys. Rev. B **55**, 15108–15118.
De'Bell, K., and J. P. Whitehead, 1991, J. Phys.: Condens. Matter **3**, 2431–2439.
De'Bell, K., and J. P. Whitehead, 1994, Physica B **194–196**, 179–180.
Dirken, M. W., and L. J. de Jongh, 1987, Solid State Commun. **64**, 1202.
Döring, W., 1961a, Z. Naturforsch. A **16a**, 1146–1152.
Döring, W., 1961b, Z. Naturforsch. A **16a**, 1008–1016.
Dunlap, B. D., M. Slaski, Z. Sungaila, D. G. Hinks, K. Zhang, C. Segre, S. K. Malik, and E. E. Alp, 1988, Phys. Rev. B **37**, 592–594.
Erickson, R. P., and D. L. Mills, 1992, Phys. Rev. B **46**, 861–865.
Farle, M., and K. Baberschke, 1987, Phys. Rev. Lett. **58**, 511–514.
Farle, M., B. Mirwald-Schulz, A. N. Ansimov, W. Platow, and K. Baberschke, 1997, Phys. Rev. B **55**, 3708–3715.
Farle, M., W. Platow, A. N. Anisimov, B. Schulz, and K. Baberschke, 1997, J. Magn. Magn. Mater. **165**, 74–77.
Fischer, P., B. Schmid, P. Breusch, F. Stucki, and P. Ulternahrer, 1989, Z. Phys. B **74**, 183–189.
Fujiki, N. M., K. De'Bell, and D. J. W. Geldart, 1987, Phys. Rev. B **36**, 8512–8516.
Garel, T., and S. Doniach, 1982, Phys. Rev. B **26**, 325–329.
Gay, J. G., and R. Richter, 1986, Phys. Rev. Lett. **56**, 2728–2731.
Gay, J. G., and R. Richter, 1987, J. Appl. Phys. **61**, 3362–3365.
Goldman, A. I., B. X. Yang, J. Tranquada, J. E. Crow, and C.-S. Jee, 1987, Phys. Rev. B **36**, 7234–7236.
Heinrich, B., and J. F. Cochran, 1994, Adv. Phys. **42**, 523–639.
Henley, C. L., 1989, Phys. Rev. Lett. **62**, 2056–2059.
Herring, C., and C. Kittel, 1951, Phys. Rev. **81**, 869.
Holstein, T., and H. Primakoff, 1940, Phys. Rev. **58**, 1098–1113.
Hucht, A., A. Moschel, and K. D. Usadel, 1995, J. Magn. Magn. Mater. **148**, 32–33.
Hucht, A., and K. D. Usadel, 1996, J. Magn. Magn. Mater. **156**, 423–424.
Hucht, A., and K. D. Usadel, 1997, Phys. Rev. B **55**, 12309–12312.
Hurley, M. M., and S. J. Singer, 1992a, Phys. Rev. B **46**, 5783–5787.
Hurley, M. M., and S. J. Singer, 1992b, J. Phys. Chem. **96**, 1938–1950.
Hurley, M. M., and S. J. Singer, 1992c, J. Phys. Chem. **96**, 1951–1956.
Hutchings, M. T., 1964, Solid State Phys. **16**, 227–273.
Jensen, P. J., and K. H. Bennemann, 1990, Phys. Rev. B **42**, 849–855.
Jensen, P. J., and K. H. Bennemann, 1992, Solid State Commun. **83**, 1057–1058.
Jones, T. L., and D. Venus, 1994, Surf. Sci. **302**, 126–140.
Kaplan, B., and G. A. Gehring, 1993, J. Magn. Magn. Mater. **128**, 111–116.
Kashuba, A., and V. L. Pokrovsky, 1993a, Phys. Rev. Lett. **70**, 3155–3158.
Kashuba, A. B., and V. L. Pokrovsky, 1993b, Phys. Rev. B **48**, 10335–10338.
Kivelson, D., S. A. Kivelson, X. Zhao, Z. Nussinov, and G. Tarjus, 1995, Physica A **219**, 27–38.
Kosterlitz, J. M., and D. J. Thouless, 1973, J. Phys. C **6**, 1181–1203.
Lee, B. W., J. M. Ferreira, Y. Dalichaouch, M. S. Torikachvili, K. N. Yang, and M. B. Maple, 1988, Phys. Rev. B **37**, 2368–2371.
Lessard, A., T. H. Moss, and W. Hubner, 1997, Phys. Rev. B **56**, 2594–2604.
Levanyuk, A. P., and N. Garcia, 1993, Phys. Rev. Lett. **70**, 1184.
Li, C., A. J. Freeman, H. J. F. Jansen, and C. L. Fu, 1990, Phys. Rev. B **42**, 5433–5442.
Li, D., M. Freitag, Z. Q. Qiu, and S. D. Bader, 1994, Phys. Rev. Lett. **72**, 3112–3115.
Liu, G., and S. D. Bader, 1990, J. Vac. Sci. Technol. A **8**, 2727.

Lorenz, R., and J. Hafner, 1995, J. Phys.: Condens. Matter **7**, L253–L259.
Löw, U., V. J. Emery, K. Fabricius, and S. A. Kievelson, 1994, Phys. Rev. Lett. **72**, 1918–1921.
Lynn, J. W., T. W. Clinton, W.-H. Li, R. W. Erwin, J. Z. Liu, K. Vandervoort, and R. N. Shelton, 1989, Phys. Rev. Lett. **63**, 2606.
MacIsaac, A. B., 1992, Master's thesis (Memorial University).
MacIsaac, A. B., 1997a, Physica A **239**, 147–155.
MacIsaac, A. B., 1997b, Ph.D. thesis (Memorial University).
MacIsaac, A. B., K. De'Bell, and J. P. Whitehead, 1998, Phys. Rev. Lett. **80**, 616–619.
MacIsaac, A. B., J. P. Whitehead, K. De'Bell, and K. S. Narayanan, 1992, Phys. Rev. B **46**, 6387–6394.
MacIsaac, A. B., J. P. Whitehead, K. De'Bell, and P. H. Poole, 1996, Phys. Rev. Lett. **77**, 739–742.
MacIsaac, A. B., J. P. Whitehead, and K. De'Bell, 2000, unpublished.
MacIsaac, A. B., J. P. Whitehead, M. C. Robinson, and K. De'Bell, 1995, Phys. Rev. B **51**, 16033–16045.
Male'ev, S. V., 1976, Sov. Phys. JETP **43**, 1240–1246.
Malletta, H., E. Porschke, T. Chattopadhyay, and P. J. Brown, 1990, Physica C **166**, 9–14.
Maple, M. B., Y. Dalichaouch, J. M. Ferreira, R. R. Hake, B. W. Lee, J. J. Neumeier, M. S. Torikachvili, K. N. Yang, and H. Zhou, 1987, Physica B **148**, 155–162.
Matsubara, T., and A. Kotani, 1984, *Superconductivity in Magnetic and Exotic Materials* (Springer, Berlin).
Mermin, N. D., and H. Wagner, 1966, Phys. Rev. Lett. **17**, 1133–1136.
Moschel, A., and K. D. Usadel, 1995, Phys. Rev. B **51**, 16111–16114.
Müller, S., P. Bayer, C. Reischl, K. Heinz, B. Feldmann, H. Zillgen, and M. Wuttig, 1995, Phys. Rev. Lett. **74**, 765–768.
Nakazawa, Y., M. Ishikawa, and T. Takabatake, 1987, Physica B **148**, 404–407.
Néel, L., 1954, J. Phys. Lett. (France) **15**, 376–378.
Pappas, D. P., K.-P. Kämper, and H. Hopster, 1990, Phys. Rev. Lett. **64**, 3179–3182.
Paul, D. Mck., H. A. Mook, L. A. Boatner, B. C. Sales, J. O. Ramey, and L. Cussen, 1988, Phys. Rev. B **39**, 4291–4294.
Pescia, D., and V. L. Pokrovsky, 1990, Phys. Rev. Lett. **65**, 2599–2601.
Pescia, D., and V. L. Pokrovsky, 1993, Phys. Rev. Lett. **70**, 1185.
Pich, C., and F. Schwabl, 1993, Phys. Rev. B **47**, 7957–7960.
Pich, C., and F. Schwabl, 1994, Phys. Rev. B **49**, 413–416.
Pick, S., J. Dorantes-Dávila, G. M. Pastor, and H. Dreyssé, 1994, Phys. Rev. B **50**, 993–997.
Pick, S., and H. Dreyssé, 1992, Phys. Rev. B **46**, 5802–5805.
Prakash, S., and C. L. Henley, 1990, Phys. Rev. B **42**, 6574–6589.
Prutton, M., 1994, *Introduction to Surface Physics* (Clarendon, Oxford).
Rappoport, T. G., F. S. D. Menezes, L. C. Sampaio, M. P. Albuquerque, and F. Mello, 1998, Int. J. Mod. Phys. C **9**, 1–5.
Reeves, M. E., D. S. Citrin, B. G. Pazol, T. A. Friedmann, and D. M. Ginsberg, 1987, Phys. Rev. B **36**, 6915–6919.
Roland, C., and R. Desai, 1990, Phys. Rev. B **42**, 6658–6677.
Sagui, C., and R. Desai, 1994, Phys. Rev. E **49**, 2225–2244.
Sampaio, L. C., M. P. Alburquerque, and F. S. de Menezes, 1996, Phys. Rev. B **54**, 6465–6472.
Saxena, A., Y. Wu, T. Lookman, S. R. Shenoy, and A. R. Bishop, 1997, Physica A **239**, 18–34.
Schulz, B., and K. Baberschke, 1994, Phys. Rev. B **50**, 13467–13471.
Seul, M., and D. Andelman, 1995, Science **267**, 476–483.
Seul, M., L. R. Monar, L. O'Gorman, and R. Wolfe, 1991, Science **254**, 1616–1618.
Seul, M., and R. Wolfe, 1992, Phys. Rev. Lett. **68**, 2460–2463.
Simizu, S., G. H. Bellesis, J. Lukin, S. A. Freidberg, H. S. Lessure, S. M. Fine, and M. Greenblatt, 1989, Phys. Rev. B **39**, 9099–9107.
Simizu, S., S. A. Friedberg, E. Hayri, and M. Greenblatt, 1987, Phys. Rev. B **36**, 7129–7132.
Speckmann, M., H. P. Oepen, and H. Ibach, 1995, Phys. Rev. Lett. **75**, 2035–2038.
Szunyogh, L., B. Újfalussy, and P. Weinberger, 1995, Phys. Rev. B **51**, 9552–9559.
Taylor, M. B., and B. L. Gyorffy, 1993, J. Phys.: Condens. Matter **5**, 4527–4562.
Toloza, J. H., F. A. Tamarit, and S. A. Cannas, 1998, Phys. Rev. B **58**, R8885–8888.
van der Berg, J., C. J. van der Beek, P. H. Kes, J. A. Mydosh, G. J. Nieuwenhuys, and L. J. de Jongh, 1987, Solid State Commun. **64**, 699–703.
Victora, R. H., and J. M. MacLaren, 1993, Phys. Rev. B **47**, 11583–11586.
Wang, D. S., R. Wu, and A. J. Freeman, 1993a, Phys. Rev. B **47**, 14932–14947.
Wang, D. S., R. Wu, and A. J. Freeman, 1993b, Phys. Rev. Lett. **70**, 869–872.
Weber, W., C. H. Back, A. Bischof, D. Pescia, and R. Allenspach, 1995, Nature (London) **374**, 788–790.
Weinert, M., R. E. Watson, and J. W. Davenport, 1985, Phys. Rev. B **32**, 2115–2119.
White, R. M., M. Sparks, and I. Ortenburger, 1965, Phys. Rev. A **139**, 450–454.
Whitehead, J. P., 1996, Phys. Essays **9**, 609.
Whitehead, J. P., and K. De'Bell, 1994, J. Phys.: Condens. Matter **6**, L731–734.
Whitehead, J. P., K. De'Bell, and A. B. MacIsaac, 1993, in *Proceedings of Quantum Field Theory and Collective Phenomena, Perugia, Italy, 1992*, edited by S. D. Lillo, F. Khanna, G. Semenoff, and P. Sodano (World Scientific, Singapore), p. 110–134.
Yafet, Y., and E. M. Gyorgy, 1988, Phys. Rev. B **38**, 9145–9151.
Yafet, Y., J. Kwo, and E. M. Gyorgy, 1986, Phys. Rev. B **33**, 6519–6522.
Yang, K. N., J. M. Ferreira, B. W. Lee, M. B. Maple, W. H. Li, J. W. Lynn, and R. W. Erwin, 1989, Phys. Rev. B **40**, 10963–10972.
Zharnikov, M., A. Dittschar, W. Kuch, C. M. Schneider, and J. Kirschner, 1996, Phys. Rev. Lett. **76**, 4620–4623.